EVALUATION OF GEOSTATISTICS AND WAVELETS FOR IDENTIFYING RELATIONS BETWEEN IMAGERY AND DIFFERENT SPATIAL RESOLUTIONS AND FOR DATA COMPRESSION

8 Jan 99

First Interim Report (RSSUSA - 4/1)

Dr Margaret A. Oliver

July 1998 to December 1999

United States Army

ENVIRONMENTAL RESEARCH OFFICE OF THE U.S. ARMY

London, England

CONTRACT NUMBER - N68171-98-M-5311

Contractor - Approved for Public Release; distribution unlimited

REPORT DOCUMENTATION PAGE

Form Approved
OMB No. 0704-0188

1. AGENCY USE ONLY (Leave blank)	2. REPORT DATE	3. REPORT TYPE AND DATES COVERED
	08.01.99	Interim Jul 98 – Dec 99

4. TITLE AND SUBTITLE
Evaluation of geostatistics and wavelets for Identifying relations between imagery and Different spatial resolutions and for data compression

5. FUNDING NUMBERS
N68171
98-M-5311

6. AUTHOR(S)
Dr M A Oliver

7. PERFORMING ORGANIZATION NAME(S) AND ADDRESS(ES)
University of Reading, Whiteknights,
Reading, RG6 2AH, UK

8. PERFORMING ORGANIZATION REPORT NUMBER
(RSSUSA-4/1)

9. SPONSORING/MONITORING AGENCY NAME(S) AND ADDRESS(ES)
USARDSG-UK, Environmental Sciences Branch
Edison House, 233 Old Marylebone Road,
London, NW1 5TH, UK

10. SPONSORING/MONITORING AGENCY REPORT NUMBER

11. SUPPLEMENTARY NOTES
Interim Report:
Summary of work to date

12a. DISTRIBUTION/AVAILABILITY STATEMENT
No limitation on distribution/availability

12b. DISTRIBUTION CODE

13. ABSTRACT (Maximum 200 words)

This is the first report of the project to apply geostatistics and wavelet analysis to part of the area chosen at Fort A.P. Hill in northeastern Virginia. This report embraces a summary of time spent at TEC, cokriging of Korean temperature data,and the comparison between geostatistics and wavelet analysis in these sections. Although this report is the first, it covers almost half of the work to be done. The cokriging of temperature in Korea is an exercise to determine whether estimates can be improved by using more information on altitude to estimate temperature with smaller error than by ordinary kriging. Wavelets and geostatistics can both be used for filtering data for data reconstruction. A comparison between the two approaches is described. It seems that wavelets provide a more accurate method for data reconstruction, but geostatistics is more appropriate for exploring different resolutions of spatial variation that have been identified by the variogram.

14. SUBJECT TERMS
Keywords: cokriging, long range component, short range component, wavelets,variogram

15. NUMBER OF PAGES

16. PRICE CODE

17. SECURITY CLASSIFICATION OF REPORT	18. SECURITY CLASSIFICATION OF THIS PAGE	19. SECURITY CLASSIFICATION OF ABSTRACT	20. LIMITATION OF ABSTRACT

NSN 7540-01-280-5500

Standard Form 298 (Rev. 2-89)
Prescribed by ANSI Std. Z39-18
298-102

Evaluation of geostatistics and wavelets for identifying relations between imagery and different spatial resolutions and for data compression

Introduction

This report embraces several aspects of the work to date. It begins with a brief summary of the work that was done by Dr Oliver at TEC in February 1997 which was part of this contract (albeit slightly premature), and the work done while E. Bosch was working with Dr Oliver at Reading in September. The majority of the report will focus on a comparison between wavelet and geostatistics as far as we have gone.

The work for most of this project will be based at Fort A. P. Hill in northeastern Virginia, about 75 miles from Washington, DC. The area is intensely dissected by many small waterways, and this appears to have contributed to the pattern of variation observed in the image. The ground cover survey data and digital elevation model will be used in a second stage of analysis.

Report of visit to TEC in January 1998

Much of the first day at TEC was spent discussing the results of the first analyses from Fort A. P. Hill, and what other work should be done. In addition the paper that has now been accepted by the International Journal of Remote Sensing was also discussed and suggestions for improvement considered and incorporated. Since Dr Oliver was to brief the senior management team at TEC including Dr Roper the contents of the briefing were also ratified at the outset.

The main aim of this visit was to work with Jim Shine to enable him to make full use of Genstat. A set of programs was prepared to cover exploratory data analysis (histograms, box plots, summary statistics, trend detection and so on), variogram analysis and modelling and kriging. All of the programs were examined. They were eventually compiled as part of the aide memoire that formed an Aapendix of the final report for the previous contract (Contract N68171-97-C-9029).

Jim Shine and Dr Oliver worked though all of the programs. A problem was identified with the kriging algorithm in Genstat which was eventually reported to the NAG library and corrected. TEC then received a new implementation of the package. At least half of the time at TEC was spent instructing Jim in the use of the programs and interpreting the results. In addition we had several discussions on geostatistics.

Half a day was spent on the briefing to Dr Roper and senior staff at TEC, and in answering questions arising from this. During the course of our collaboration we have covered a substantial amount of work and much of it was described briefly at this meeting. Dr Roper showed considerable interest in what has been done and when he visited the University of Reading in November 1998 it was clear that he had a sound

appreciation of the value of geostatistical analysis. The discussion that followed the briefing was stimulating and well considered.

Other discussions were held with Edward Bosch about comparing wavelets and geostatistics. This culminated with an arrangement for him to visit Reading in September 1998.

Dr Oliver and E. Bosch worked together for a week. The time was used for analyses, interpreting results and discussion. Several analyses were undertaken - some of which feature in the report. Others have been done by both of us subsequently. The visit was very profitable to both of us. As a result of this investigation we have submitted an abstract to the Geostatistics Congress to be held in April 2000. This is appended at the end of the report. The paper, if accepted, will acknowledge the support of US Army and of TEC in this work, and will be authored jointly by M. A. Oliver, E. Bosch and K. Slocum.

Comparing wavelets and kriging for exploring nested scales of variation

This work has continued to use part of the SPOT image around Anderson Camp. However, it is slightly different in extent from that used previously to accommodate the wavelet analysis. This analysis works better if the area analysed is some factor of 2; the area chosen was 2^7. As a result the variogram analysis and factorial kriging had to be redone so that the results relate to this new region and are comparable with all subsequent analyses. The theory of factorial kriging was given in the final report for Project 3 (Contract number N68171-97-C-9029). The theory of factorial kriging was also given in the paper presented at the geoENV98 conference which has already been submitted to TEC. I shall summarise the application of wavelets, but with little theory as this is not my field and Edward Bosch is the local expert at TEC.

Summary of wavelet analysis

The wavelet transform has some similarity with the Fourier and the windowed Fourier transforms. However, the wavelet transform is localized in terms of frequency and scale (via dilations) and in time (via translations), whereas the Fourier transform, although localized in frequency, is not localized in time or space. The windowed Fourier transform operates more locally. The advantage of the wavelet transform over the windowed Fourier transform is that low frequency and high frequency resolutions can be characterized simultaneously. This means that wavelet analysis is suitable for situations where there are different levels of variation superimposed on each other (Daubechies, 1992). Wavelets are also good for describing transient data whereas the Fourier transform is not. Wavelet analysis is not affected by local non-stationarity and this is an advantage it has compared with geostatistics, which assumes that the data are at least quasi-stationary (i.e. locally stationary). Local non-stationarity can arise where there are marked boundaries that result in a marked change in the local means of the variable of interest.

Wavelets are oscillatory components that operate locally. The wavelet analysis starts with the choice of a mother wavelet, $w(t)$, which is fixed. The mother wavelet can be dilated or shrunk to examine components in the variation that occur at different spatial or temporal scales. This enables multi-resolution analysis where different levels of variation are superimposed on one another (Mallat, 1998). This is our first aim in this investigation. Redundancy is a major problem with image data because of the amount of information involved. Wavelets are also of great value for data compression because they are able to remove and to retain the important structure.

Theory

Wavelet analysis allows a signal (information) to be represented in terms of a set of basis functions, i.e. basis vectors or kernels. The basis functions are a set of linearly independent functions that can be used to produce all admissible functions of $f(t)$ (Strang and Nguyen, 1996). Choosing the basis functions determines the kind of information that can be extracted.

$$f(t) = \Sigma b_{su} w_{su}(t) \qquad (1)$$

where b_{su} are the coefficients for scaling (s) and translation (u). The special feature of the wavelet basis is that all functions $w_{su}(t)$ are constructed from a single mother wavelet $w(t)$. If the wavelet normally starts at $t = 0$ and ends at $t = N$, then shifted wavlets, $w_{0u}(t)$, start at $t = u$ and end at $t = u+N$. The rescaled wavelets, $ws_0(t)$, start at $t=0$ and end at $t= N/2^j$, and are translated to the right by s and compressed by a factor of 2^j. A typical wavelet w_{su} is compressed j times and shifted u times:

$$w_{su}(t) = w(2^s t - k) \qquad (2)$$

Most wavelets are orthogonal and

$$\int_{-\infty}^{\infty} w_{su}(t) w_{SU}(t) dt = 0 \qquad (3)$$

This leads to a simple formula for each coefficient b_{SU} in the expansion of $f(t)$. The expansion in equation (1) is mutiplied by w_{JK} and integrated by:

$$\int_{-\infty}^{\infty} f(t) w_{SU}(t) dt = b_{SU} \int_{-\infty}^{\infty} (w_{SU}(t))^2 dt. \qquad (4)$$

All other terms disappear because of the orthogonality.

Multiresolution

The high frequency filter leads to $w(t)$ and the low frequency one to the scaling function $\phi(t)$. In most wavelet analyses the low frequency filter is applied first and the scaling function is obtained before the wavelet. The wavelet follows from $\phi(t)$ by one application of the high frequency filter. Therefore, the scaling functions average or smooth the data while the detail in the signal is retained in the wavelets. The scaling functions and wavelets comprise the components of the multi-resolution situation which enables wavelet analysis to examine features locally at different scales. At a given resolution the scaling functions $\phi(2^s t - u)$ are a basis for the set of signals. The level is set by s, and the steps at the level are 2^{-s}. The new detail at the level s is represented by the wavelets $w(2^s t - u)$.

Strang and Nguyen (1996) represent this as follows:

signal at level s (local averages) ↘
+ → signal at level $s+1$
details at level s (local differences) ↗

Thus the signal, such as the NIR information from an image, can be divided into different scales of resolution by wavelet analysis. Multiresolution divides the frequencies into octave bands, from w to $2w$, rather than different frequencies.

The construction of wavelets starts with vectors. Every second vector xy is a combination of the basis vectors (1,0) and (0,1) (Strang, 1989). The original data are transformed by the wavelet coefficients which are both additive and orthogonal. The coefficients provide us with a measure of the energy the basis vector has at time t or scale s. The wavelet transform decomposes the signal to a basis (set) of elementary signals. It uses smaller windows at higher frequencies and larger ones at low frequencies. This means that, in essence, the analysis is based on a pair of filters - one of low frequency which smooths the data and the other is high frequency and fine which is related to the wavelet. The low frequency filter produces the scaling coefficients and the high frequency one the wavelet coefficients.

The wavelet is a function of zero average:

$$\int_{-x}^{+x} \psi(t)\mathrm{d}t = 0 \qquad (5)$$

which is dilated or compressed with a scale parameter, s, and translated by u. The wavelet coefficient $wf(u,s)$ measures the variation of f in a neighbourhood u whose size is proportional to s. The method assumes a finite variance.

There are many different kinds of wavelets, the most simple is the Haar, but probably the most popular at the moment are those of Daubechies (Daubechies, 1988).

Analysis of the A.P. Hill data

SPOT Image

The part of the scene covering Fort A. P. Hill, Figure 1, is slightly smaller than that used before (see report N68171-97-C-9029), but it covers the same part of the image. Analyses were carried out on the complete data set and on sub-samples of 1 pixel in 2 for each column and row (or 1 pixel from a block of 4), 1 pixel in 4 for each row and column (1 pixel from a block of 16), and 1 pixel in 8 for each row and column (1 pixel from a block of 64 pixels). The sub-sets were used to assess the accuracy of data reconstruction by the two methods. Table 1 gives the summary statistics for the full data set.

Table 1: Summary statistics for NIR for the 128 pixels by 128 pixels region of Fort A. P. Hill

Statistic	NIR	Hermite polynomials of NIR
Count	16384.0	16384.0
Minimum	37.00	-4.496
Maximum	183.00	4.009
Mean	117.83	0.0287
Variance	268.99	0.9995
Standard deviation	16.401	0.9997
Skewness	-0.7408	-0.0943

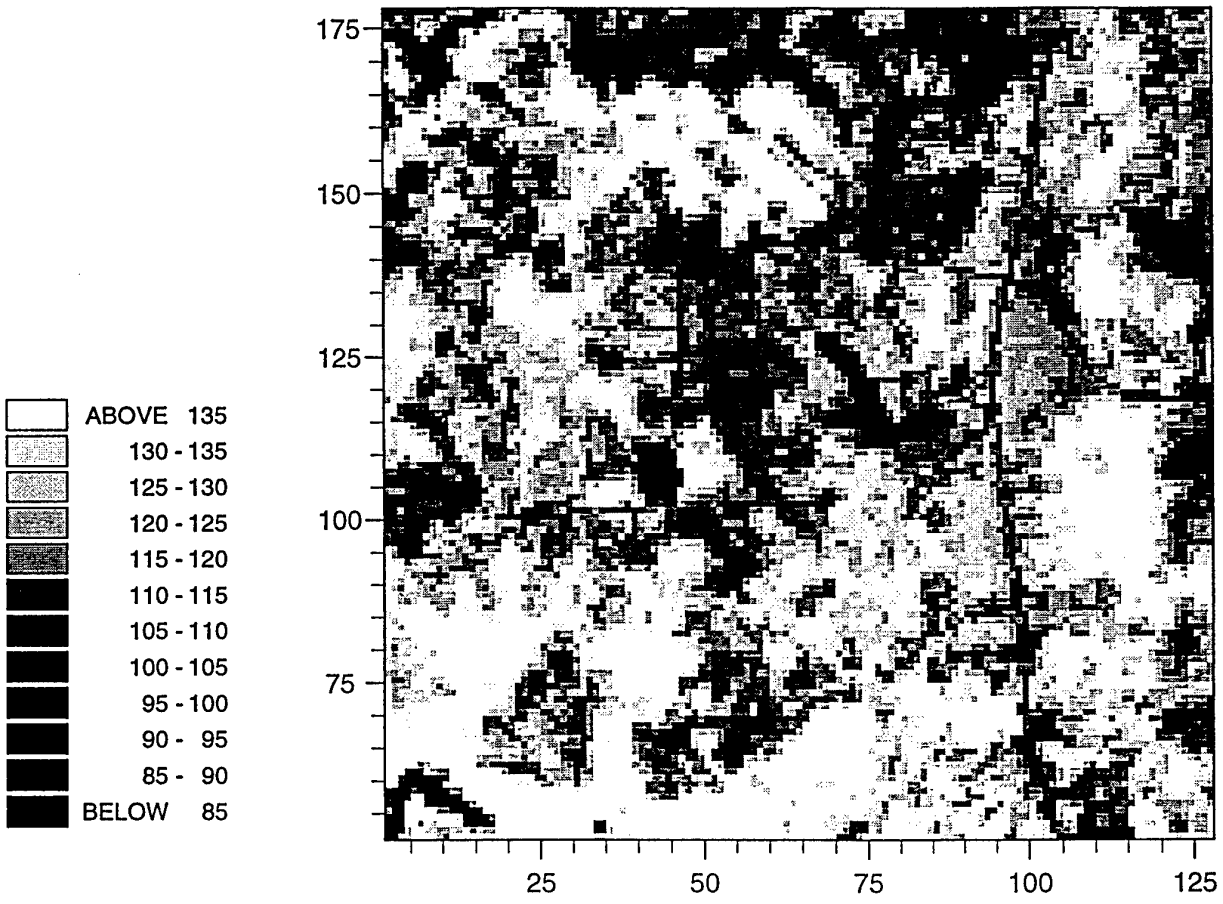

Figure 1: Pixel map of the near infra read (NIR) of part of the SPOT image (128 by 128 pixels) for Fort A. P. Hill

Wavelet analysis

The method of wavelet analysis that Edward Bosch used was that of Daubechies wavelets (Daubechies, 1988). The size of the image was 2^7, i.e. 128 rows and 128 columns of pixel information for the NIR waveband. This region was chosen from the part of the SPOT image that we analysed and described in the previous report (1998), and the size was such to avoid any need to pad the data to create appropriate resolution levels for the wavelet analysis.

The wavelet transform was done with a pair of filters and not the wavelets themselves. The signal is convolved by the filter - the result is that every other point in the output of each convolution is discarded. The convolutions can be represented in terms of two matrices **L** and **H**. The matrix **L** is made up of shifts of the low frequency filter, and **H** is made up of shifts of the high frequency filter. Since the wavelets are orthogonal:

$$\mathbf{H'H + L'L = I}$$

where $\mathbf{H'}$ is the transpose of **H**, $\mathbf{L'}$ is the transpose of **L**, and **I** is the identity matrix. The matrices **H** and **L** correspond to the forward wavelet, and $\mathbf{H'}$ and $\mathbf{L'}$ to the inverse wavelet transform. If the vector f is the frequency (NIR in our analysis), then the low frequency component of the variation in f is contained in $\mathbf{L}f$, and the high frequency component in $\mathbf{H}f$.

$$\mathbf{L'}(\mathbf{L}f) + \mathbf{H'}(\mathbf{H}f) = (\mathbf{L'\,L})f + (\mathbf{H'\,H})f = (\mathbf{L'\,L}) + (\mathbf{H'\,H})f = \mathbf{I}f = f.$$

The vectors $\mathbf{L}f$ and $\mathbf{H}f$ contain half of the number of samples as in the original set of data for f.

The filters were constructed so that there were three orthogonal filters and three vanishing moments were satisfied. The more vanishing moments there are the greater the smoothing (Daubechies, 1992). With three vanishing moments the high pass filter zeros out leaving behind little information. Most of the 'energy' or information is then retained by the low pass filter. The scaling coefficients from the low pass filter contain most of the information and it these that were used to reconstruct the image.

If the discrete wavelet transform (DWT) is applied once to the data the resolution becomes 2^6, i.e. resolution 6. This results in four quarter sets of data of size 64 by 64 pixels. The first quarter of the data represent in essence a sample of 1 in 2 of the rows and columns of the data matrix. This quarter contains the scaling coefficients which correspond to the low pass filter. The other three quarters contain the wavelet coefficients which are high frequency: quarter two contains the vertical coefficients, quarter 3 the horizontal ones and quarter 4 the diagonal coefficients.

The image information on NIR was reconstructed by an inverse wavelet transform. For this analysis the low and high frequency components were reconstructed separately. For the low frequency reconstruction:

$$fl = \mathbf{L}'(\mathbf{L}f) + \mathbf{O}'(\mathbf{H}f) = \mathbf{L}'(\mathbf{L}f),$$

where **O** is the zero matrix. Therefore, *fl* represents the reconstructed values of NIR without the high frequency information. For the high frequency reconstruction:

$$fh = \mathbf{O}'(\mathbf{L}f) + \mathbf{H}'(\mathbf{H}f) = \mathbf{H}'(\mathbf{H}f),$$

where *fh* is the high frequency information only. Therefore:

$$f = fl + fh.$$

Geostatistical analyses

The variogram was computed and modelled as usual using the smaller data set with a total of 16 384 pixels, Figure 1. This variogram was then used with the pixel information to filter the information by factorial kriging into the long-range and short-range components. Ordinary kriging was used to estimate the values of NIR at positions where pixels had been removed from the data. In other words the estimates coincided with the locations of the original values so that a direct comparison could be made between the estimates and these.

Results

The variogram for the new data is still a nested structure, but the correlation ranges are smaller than for the larger part of the scene that we investigated before. The model fitted was a nested spherical function with two structures. Since the variogram was somewhat wavy at the longer lags, to improve the fit I modelled it to a lag of 40 only. The short-range structure was 6.6 pixels or 130 m and the long-range structure was 21 pixels or 420 m. The experimental variogram (points) and the fitted model (line) are given in Figure 2 a. The parameters of the models fitted to 100 and to 40 lags are given in Table 2. Since the data were skewed I transformed them using Hermite polynomials and computed the variogram from the transformed data, Figure 2b and Table 2. There was little difference from the raw variogram, therefore, I did the analyses on the raw data.

a)

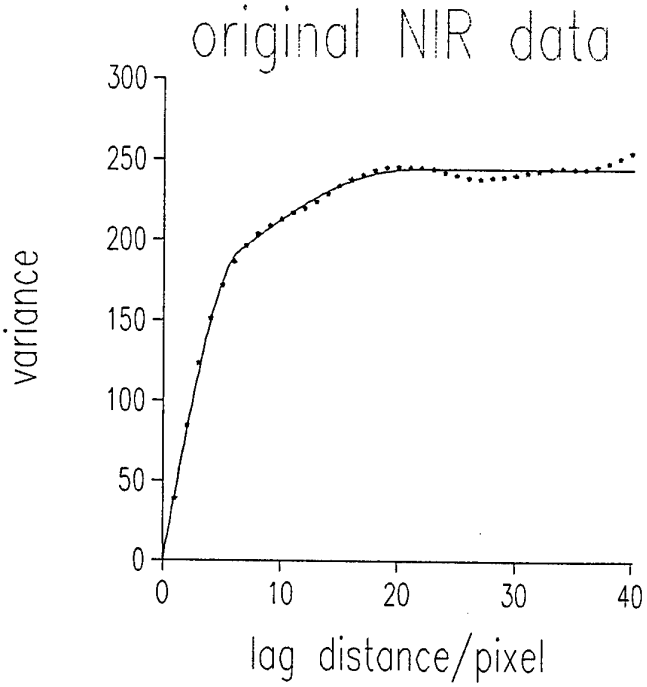

b)

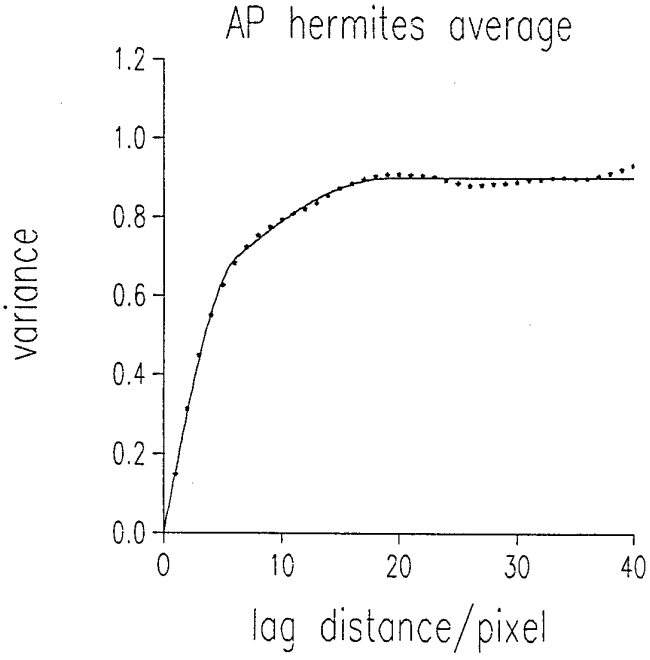

Figure 2: a) Variogram of the near infra read (NIR) of part of the SPOT image (128 by 128 pixels) for Fort A. P. Hill, b) variogram of the transformed pixel data using Hermite polynomials

Multiresolution analysis (filtering)

The variogram suggests that there are two clear scales of spatial variation present: one of about 120 m and the other of about 420. This is also evident in the pixel map of the ordinary kriged estimates, Figure 3. There is local detailed variation superimposed on a broader pattern of variation. The major large structures in the variation that are evident appear to be related to major relief forms: the drainage basins and the intervening spurs, and the major types of ground cover. Short-range variation is also evident related to the water bodies, buildings and the more local changes in ground cover and drainage. These were described in the previous final report.

Table 2: Model parameters for the variograms computed for the 128 by 128 pixel area of the SPOT image

Variable	Model type	Nugget variance	Sill(1) variance	Range(1) pixels (m)	Sill(2) variance	Range(2) pixels (m)
NIR (100 lags)	Nested Exponential	0.0	227.0	13.2 (264)	4.40	85.1 (1701.6)
NIR (40 lags)	Nested Spherical	0.0	152.2	6.46 (130)	91.71	21.11 (420)
Hermite polynomials	Nested Spherical	0.0	0.5240	6.21 (125)	0.3755	19.45 (390)
Long-range component	Circular	0.0	113.9	17.2 (544)		
Short-range component	Spherical	0.0	87.9	4.30 (86)		
Low frequ -ency 1 in 2	Nested Spherical	0.0	146.7	8.40 (168)	74.82	22.2 (444)
High frequ -ency 1 in 2	Pure nugget					
High frequ -ency 1 in 4	Circular	0.0	41.7	2.944 (58.88)		
High frequ -ency 1 in 8	Circular	0.0	68.30	6.690 (133.8)		

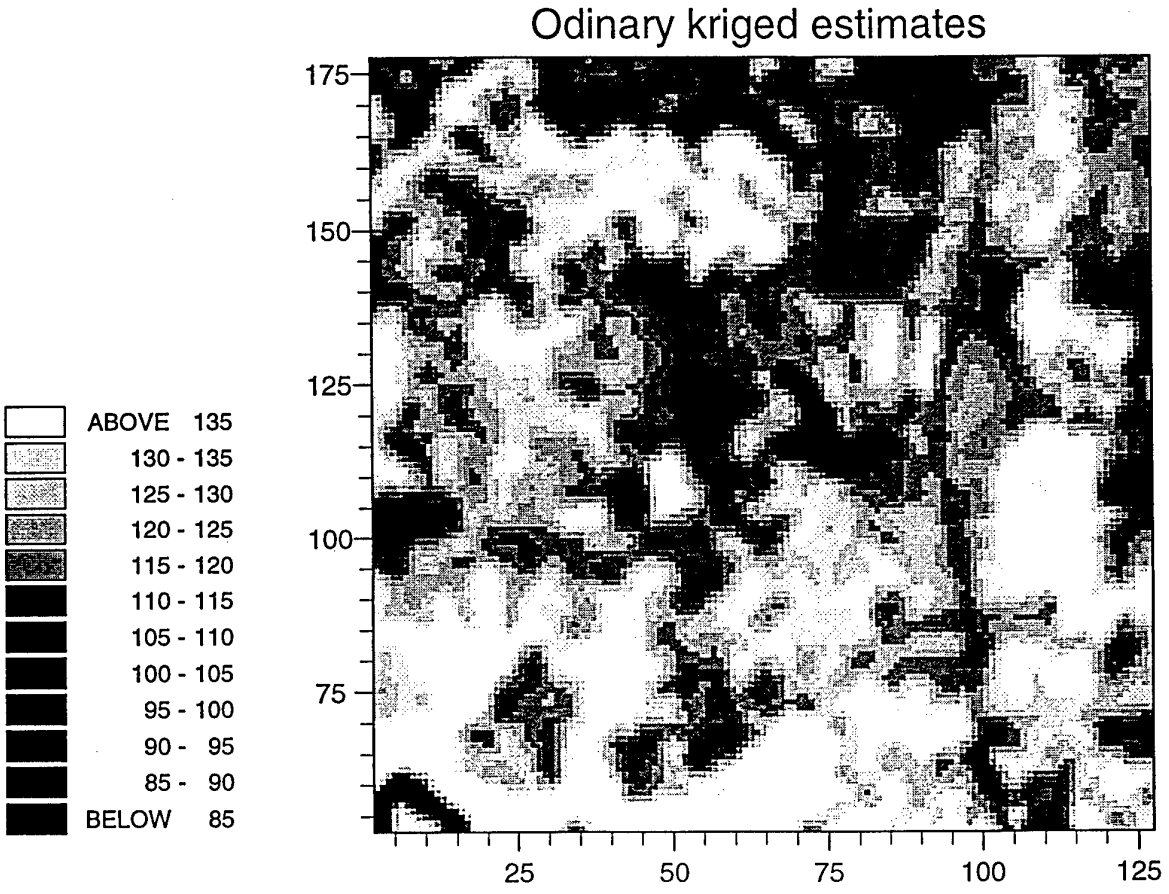

Figure 3: Pixel map of the kriged NIR of part of the SPOT image (128 by 128 pixels) for Fort A. P. Hill

Factorial kriging and wavelet analysis enable the different spatial scales to be separated in theory. For factorial kriging this is controlled by the variogram which describes the variation present in the data. For the wavelet analysis this is controlled by the resolution level which is controlled by the octave bands and as a consequence is more arbitrary. One aspect of future research is to consider how the variogram could be used to guide the factoring process that controls the wavelet multiresolution analysis.

Figure 4 is a pixel map of the kriged estimates of the long-range component of the variation filtered using the variogram. The large scale variation is related to the main relief features. The band of dark colours in the North and central part of the map are damper and wetter areas, and the lighter ones the spurs, upper slopes and built areas. This map could be used effectively to guide future sampling. If the end-user is interested in retrieving this level of information then a suitable sampling interval can be chosen using the range of the variogram. A sampling interval of 200 m would be adequate to ensure that this resolution of variation is identified.

The pixel map of the short-range variation (Figure 5) shows the detail that is also evident in Figure 3, but less clearly so. The lakes are recovered well by this resolution. The dark patches in the bottom left hand corner (1 to 20 on the x-axis and 55 to 60 on the y-axis), in the central area (64 to 90 on the x-axis and 115 to 125 on the y-axis), and at the top of the map (45 to 70 on the x-axis and 158 to 180 on the y-axis). The road running N-S is also evident extending N along longitude 100 (on this map). The other short-range structures probably relate to changes in local drainage conditions and vegetation. For many surveys recovering this intensity of variation at a scale of about 120 m would require too much sampling. A sampling interval of 50 m to 60 m would be needed to resolve this short-range variation. If a sampling scheme of about 200 m were recommended in relation to the long-range variation this information on short-range variation would be lost. These maps enable us to demonstrate to the end-user the extent of information that is likely to be lost by adopting the coarser sampling. Sampling between 60 m and 200 m would be of little benefit because most of the short-range variation would not be identified and sampling at less than 200 m would be inefficient to identify the long-range variation. Variograms were computed from the estimates of the long-range (Figure 6a) and the short-range (Figure 6b) components. They recover the spatial scale of the variation quite well, but both variograms were difficult to model satisfactorily.

For the first wavelet analysis the level of resolution was 2^6. The coefficients were derived as described earlier. The low frequency and the high frequency coefficients were reconstructed by the inverse wavelet transform, which restored each of the 64 by 64 sets coefficients to the size of the original data set. These are shown as pixel maps and should be compared with the appropriate kriged and the filtered maps, Figures 3 to 5. In addition variograms were computed for each of these reconstructions: low frequency (Figure 7a) and high frequency (Figure 7b).

The low frequency reconstruction, Figure 8, is very similar to the ordinary kriged output for the image, Figure 3. It is important to remember that the ordinary kriged

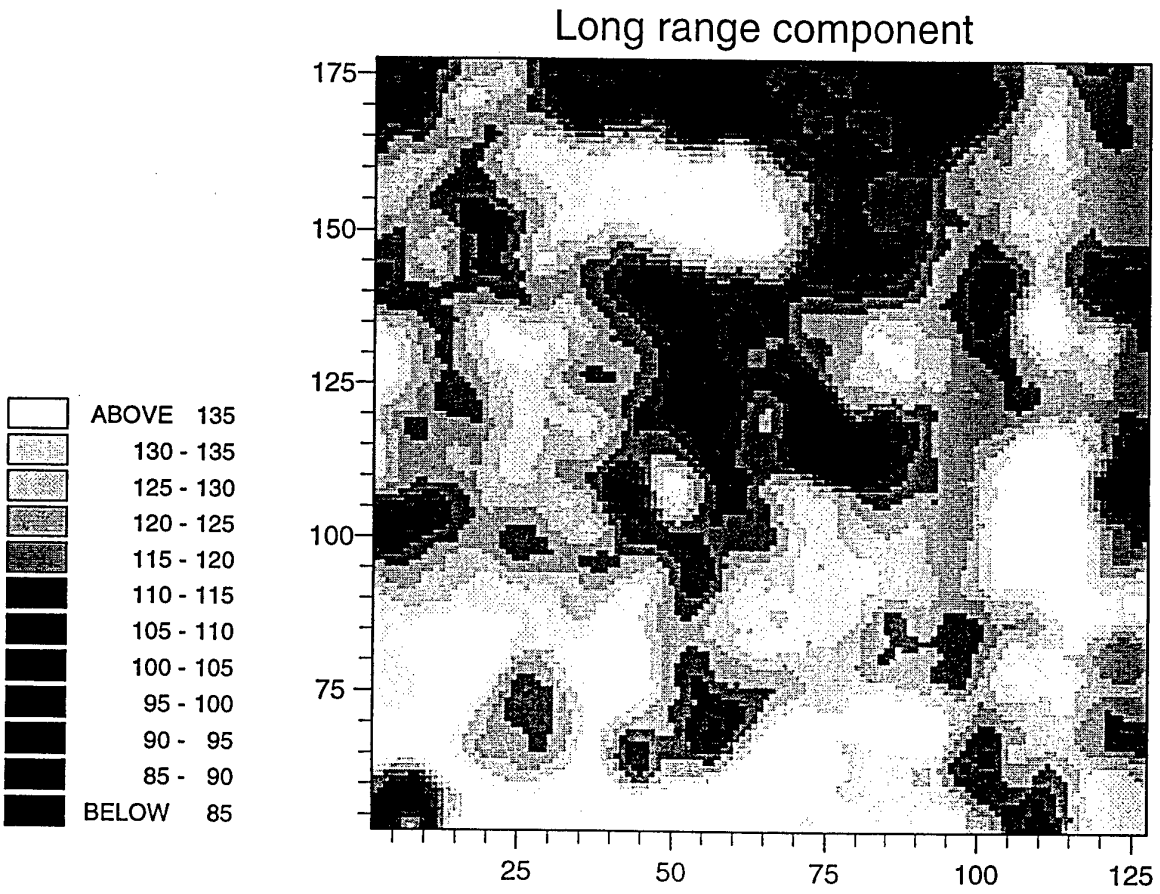

Figure 4: Pixel map of the long-range component of the variation in NIR of part of the SPOT image (128 by 128 pixels) for Fort A. P. Hill

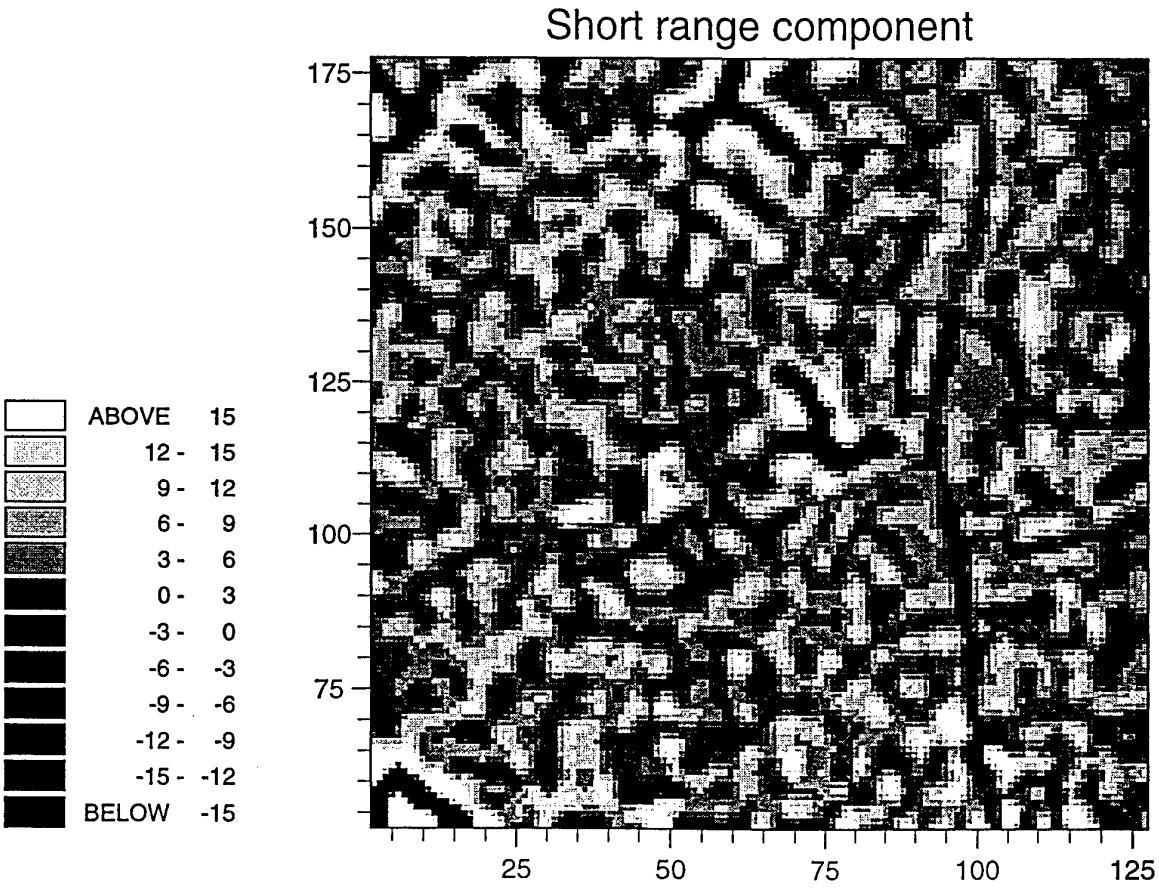

Figure 5: Pixel map of the short-range component of the variation in NIR of part of the SPOT image (128 by 128 pixels) for Fort A. P. Hill

a)

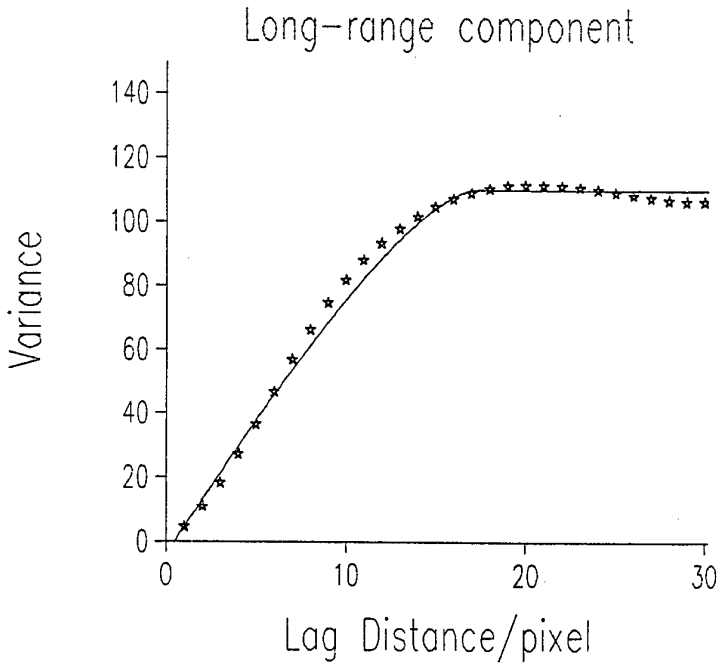

b)

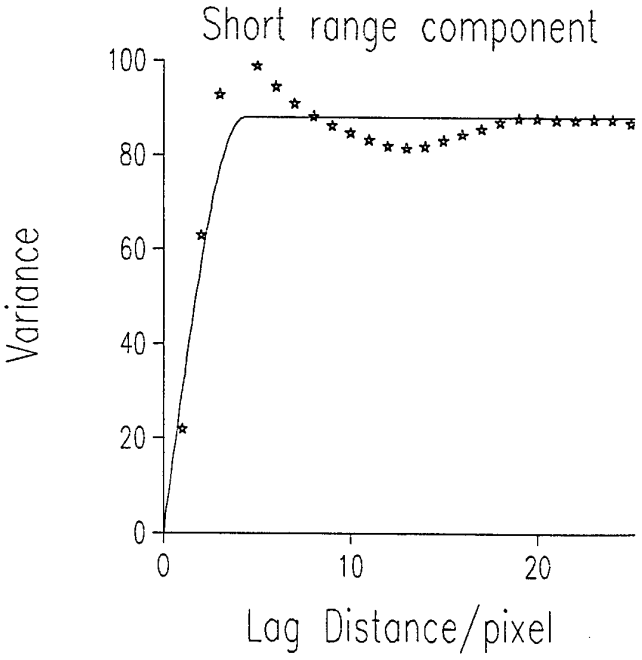

Figure 6: a) Variogram of the long-range component, and b) variogram of the short-range component of the variation in NIR of part of the SPOT image (128 by 128 pixels) for Fort A. P. Hill

a)

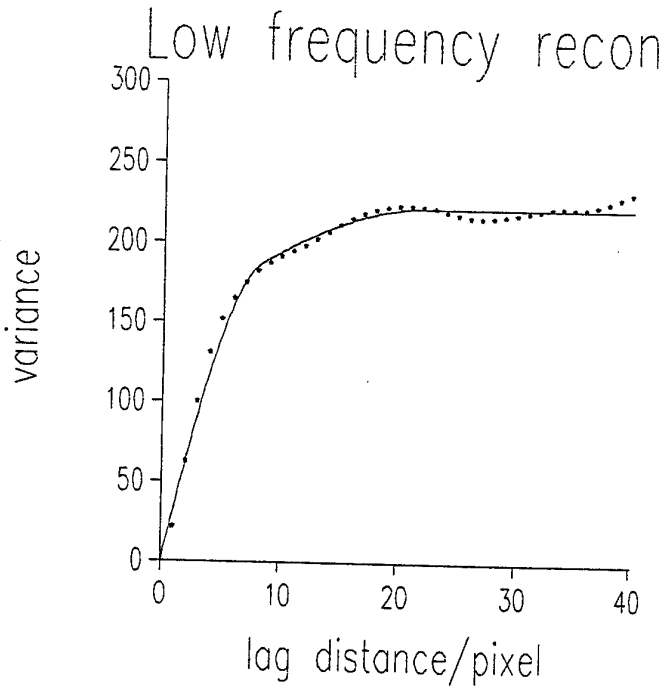

b)

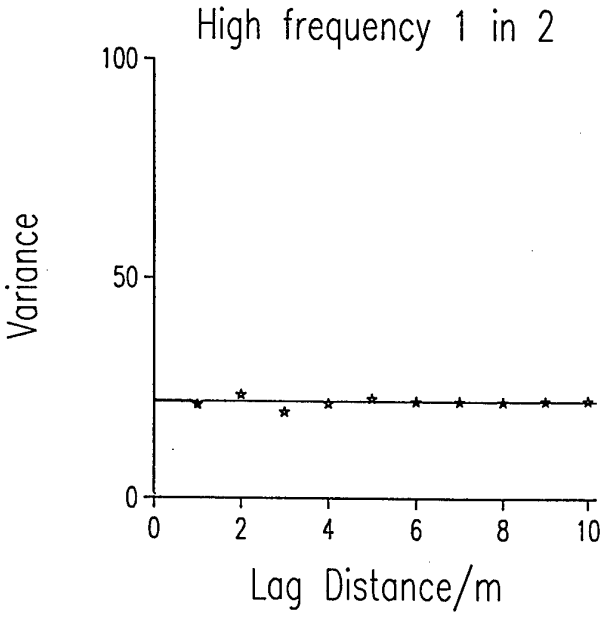

Figure 7: a) Variogram of the low-frequency component, and b) variogram of the high-frequency component of the variation in NIR of part of the SPOT image (128 by 128 pixels) for Fort A. P. Hill from a wavelet analysis at a resolution of 1 in2

map was made from estimates using all of the data, whereas the low frequency wavelet reconstruction used the 1 in 2 sample, i.e. 25% of the original data. Both the long- and short-range components of the variation are evident, although there has been some loss of detail in the short-range variation. For example the road is less clear in Figure 8 than in Figure 3. The variogram computed from the low frequency reconstruction, Figure 7a, was very similar to the variogram of the raw data, Figure 2a. Hence the spatial structure at both scales has been retained at this level of resolution. The most surprising finding was that related to the high frequency reconstruction. The map of the high frequency component (Figure 9) does not appear to reflect the kind of variation present in the map of the short-range component from factorial kriging. However, when we examined them in detail there is some weak evidence of the lakes, which are very clear in Figure 5, and the road. The variogram computed from these data is pure nugget, Figure 7b, which means that the high frequency components are noise at this level of resolution; they contain no spatial structure. The latter is all retained in the low frequency reconstruction.

To determine whether we could retrieve the long- and short-range components using wavelets we explored the next resolution, 2^5, in effect a sampling of 1 in 4 (or 1 pixel in 16). Figure 10 shows the low frequency reconstruction. There is still long- and short-range variation evident, although the short range variation is becoming less distinct; for example the road and the lakes are still visible but their margins are less clearly defined. Figure 11 shows the pixel map for the average of the high frequency reconstruction and it is clear that there is more of the short-range component of the variation evident. The variogram of the high frequency reconstruction now shows some structure, Figure 12a. Table 2 gives the model parameters of this variogram.

The low frequency reconstruction of the 1 in 8 resolution 2^4 now shows the long-range component of the variation identified by factorial kriging, Figure 13. This resolution is fairly close to the short-range component of the variogram, i.e. 6.5 pixels, and this level of variation appears to have been filtered out now. So it seems that once the resolution of the short-range structure has been reached the effect was to remove the short-range variation. The map, Figure 14, of the high frequency reconstruction now shows some of the features evident in the kriged map of the short-range component of the variation. In particular the lakes are evident. The variogram computed from the average of the three high frequency reconstructions, Figure 12b, shows clear evidence of structure and the range of spatial correlation described, 6.69 pixels, is close to the short-range component of the variogram of the original data.

Summary

It is clear that factorial kriging works well with multiresolution data. The main reason for this is that the filtering is controlled by the variogram which is a function of the data being analysed. It is a valuable method for directing future sampling for ground surveys because it can show what degree of variation is likely to be recovered. The multiresolution analysis using wavelets produces a different outcome. At the first resolution the high frequency components remove the noise, i.e spatially uncorrelated

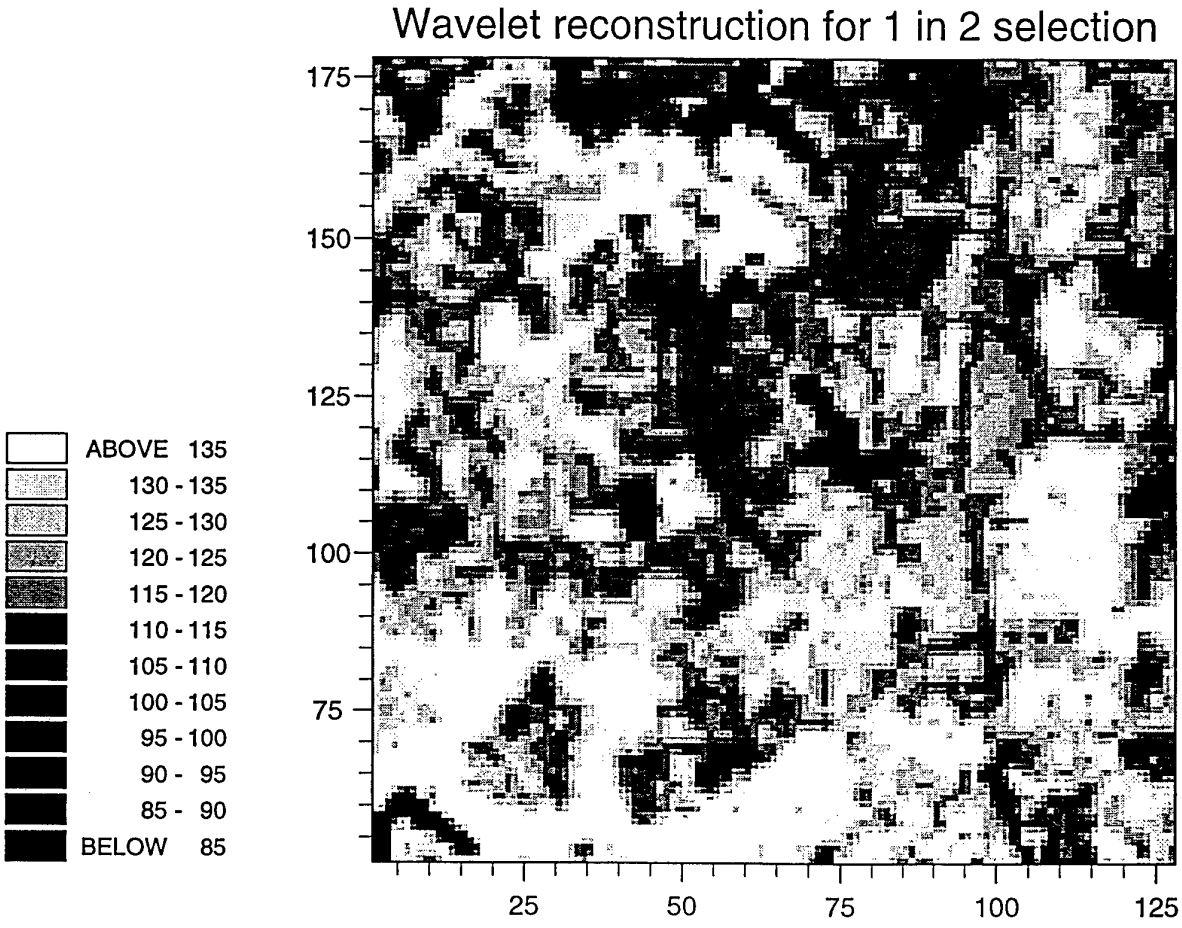

Figure 8: Pixel map of the low frequency reconstruction from the wavelet analysis of NIR of part of the SPOT image (128 by 128 pixels) for Fort A. P. Hill at a resolution of 1 in 2

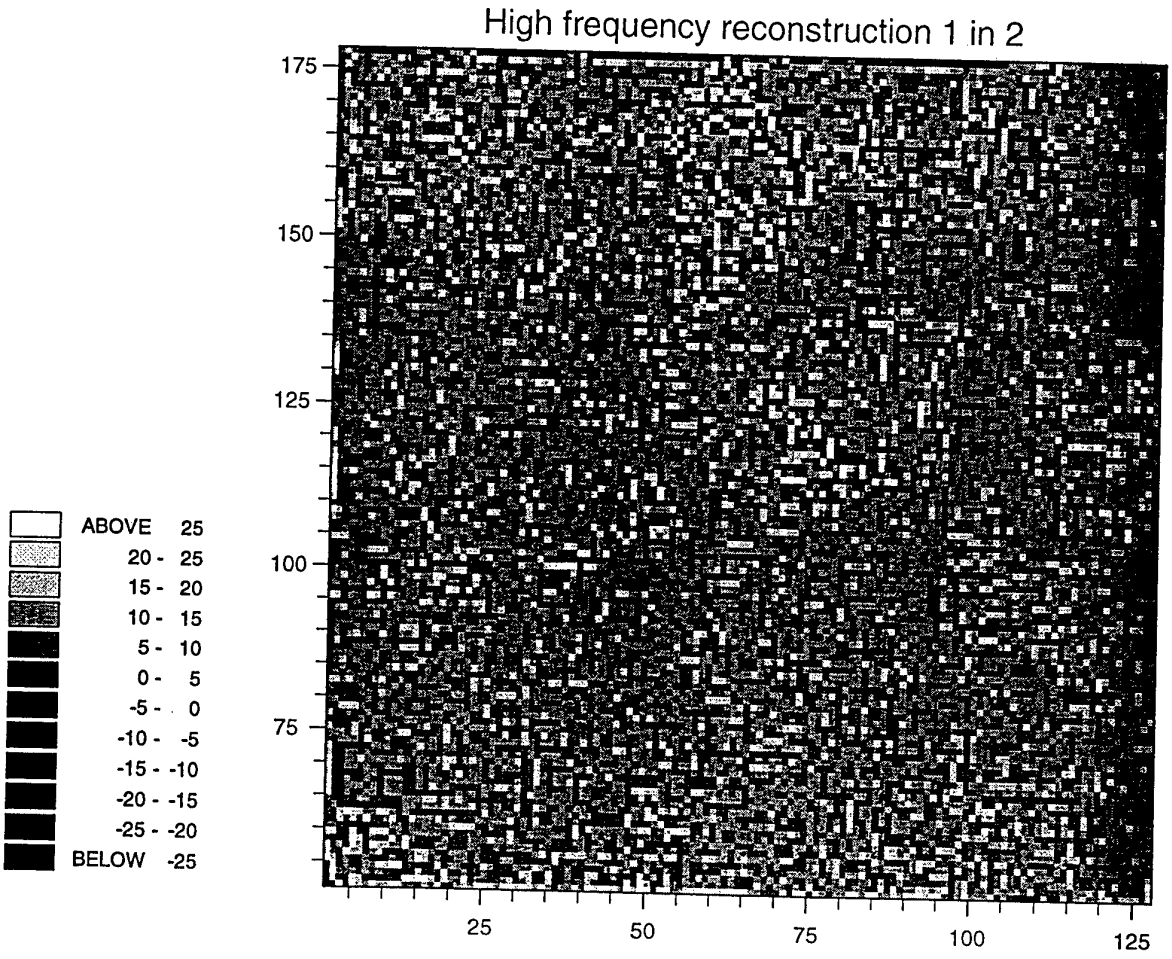

Figure 9: Pixel map of the average reconstruction of the high frequency wavelets from the wavelet analysis of NIR of part of the SPOT image (128 by 128 pixels) for Fort A. P. Hill at a resolution of 1 in 2

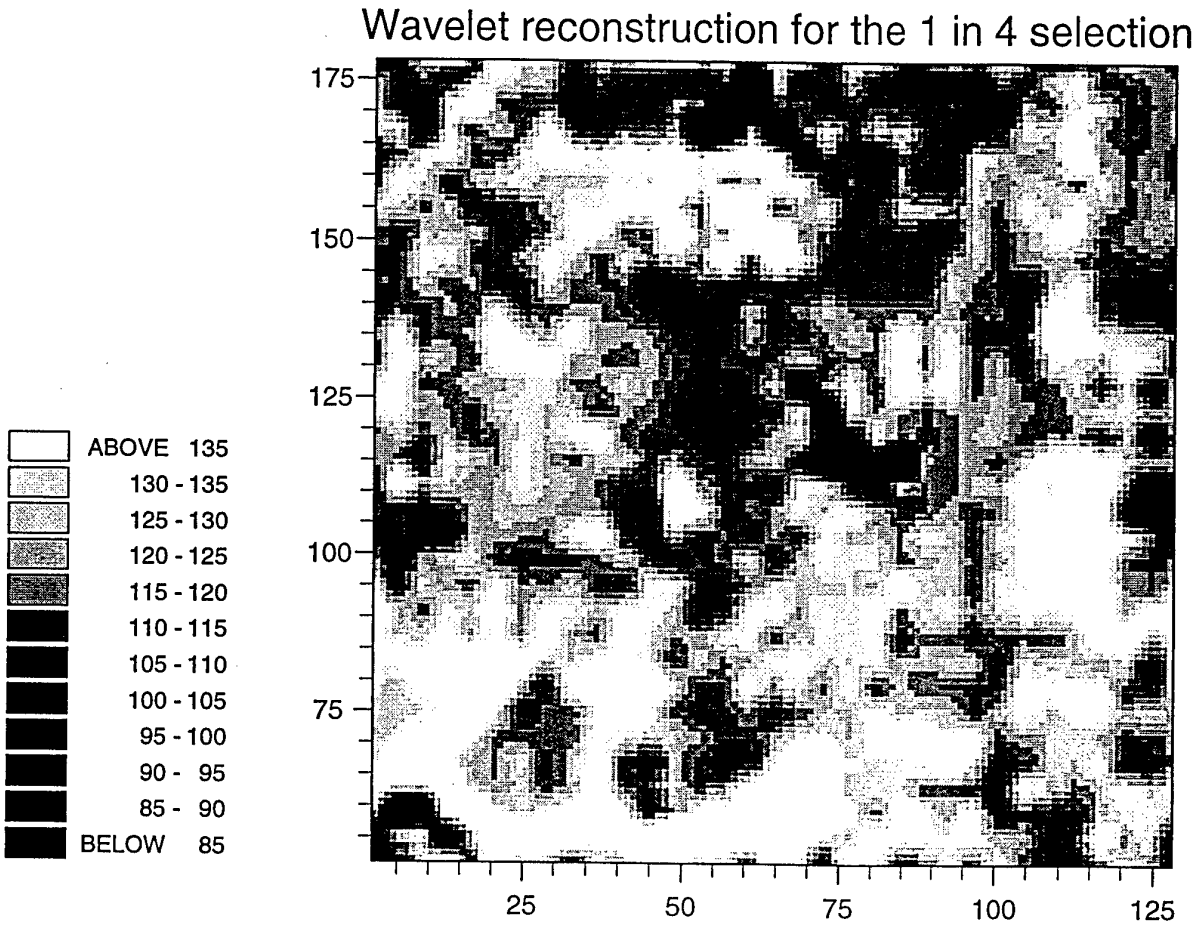

Figure 10: Pixel map of the low frequency reconstruction from the wavelet analysis of NIR of part of the SPOT image (128 by 128 pixels) for Fort A. P. Hill at a resolution of 1 in 4

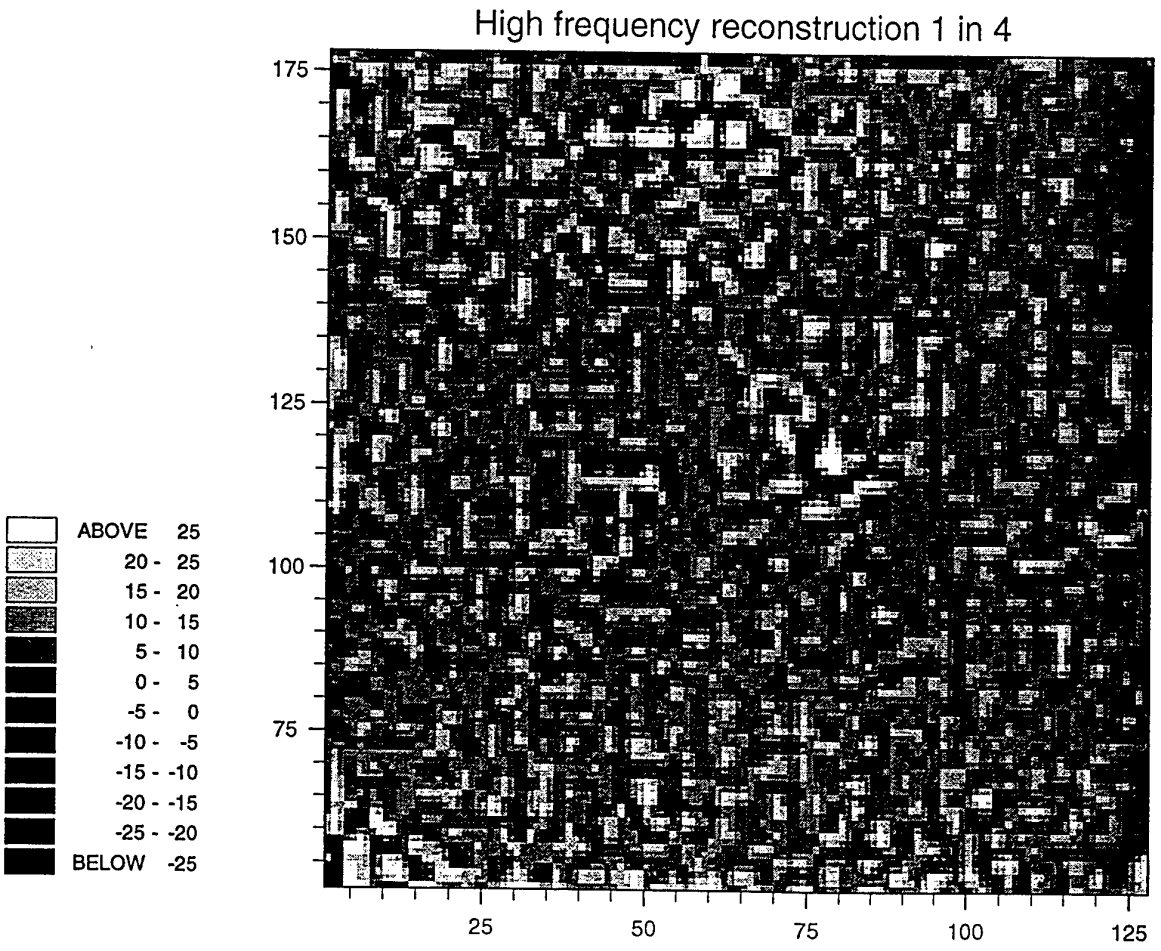

Figure 11: Pixel map of the average high frequency reconstruction from the wavelet analysis of NIR of part of the SPOT image (128 by 128 pixels) for Fort A. P. Hill at a resolution of 1 in 4

a)

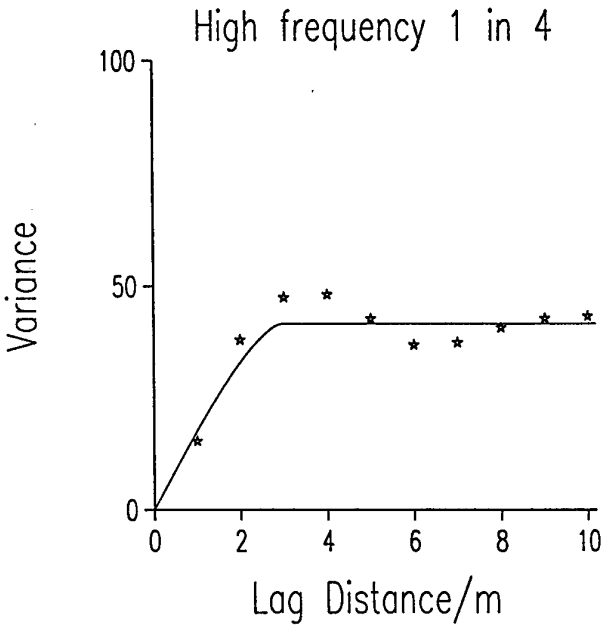

b)

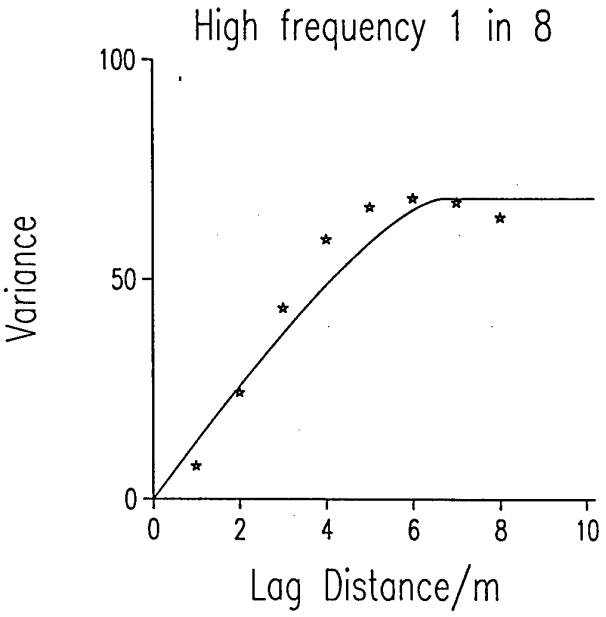

Figure 12: a) Variogram of the high-frequency component for the 1 in 4 resolution, and b) variogram of the high-frequency component for the 1 in 8 from the wavelet analysis of NIT at Fort A. P. Hill

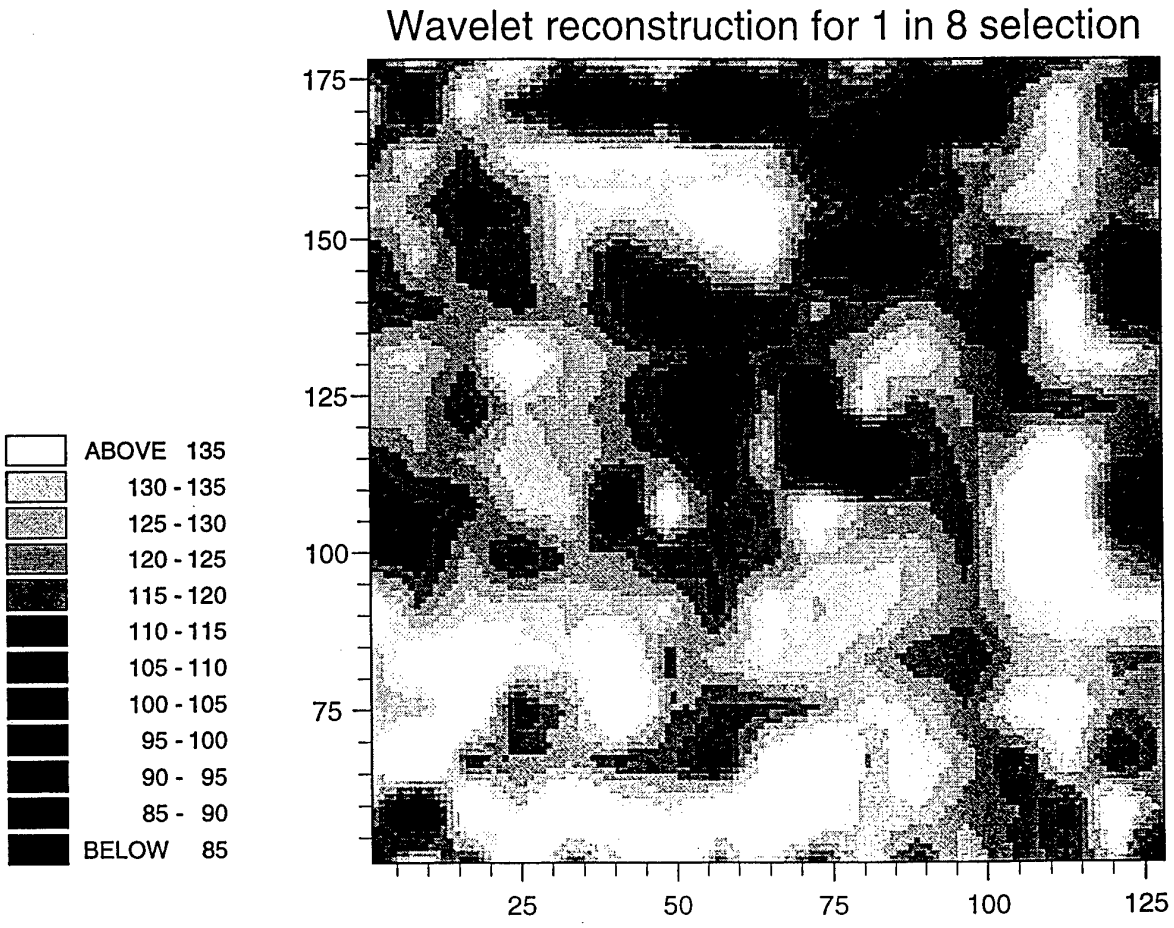

Figure 13: Pixel map of the low frequency reconstruction from the wavelet analysis of NIR of part of the SPOT image (128 by 128 pixels) for Fort A. P. Hill at a resolution of 1 in 8

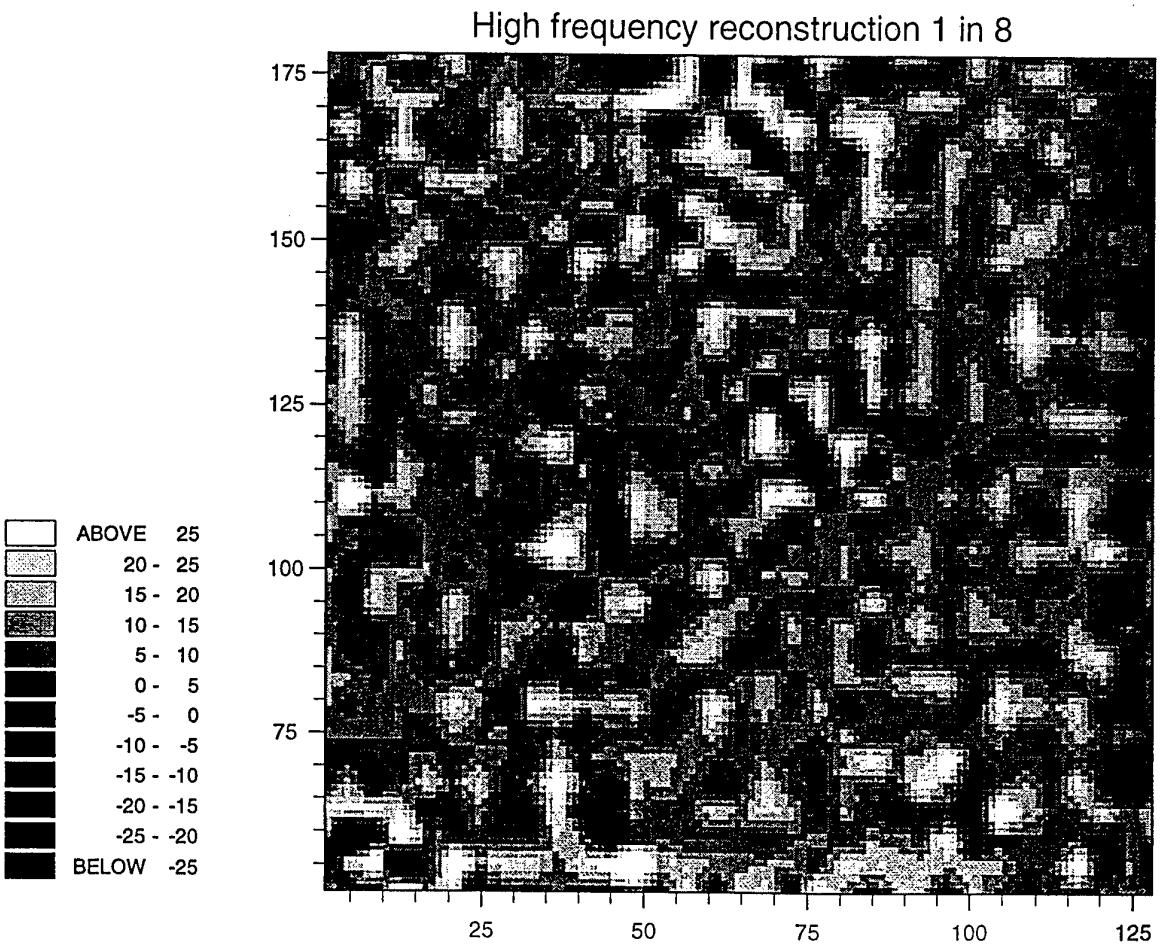

Figure 14: Pixel map of the average high frequency reconstruction from the wavelet analysis of NIR of part of the SPOT image (128 by 128 pixels) for Fort A. P. Hill at a resolution of 1 in 8

Data reconstruction

The 128 by 128 pixels were sampled by taking one pixel in every two for each row and column (or a sample of 1 in 4) which matches the first level of resolution in the wavelet analysis 2^6, one pixel in every four for every row and column (or a sample of 1 in 16), a wavelet resolution of 2^5, and one pixel in every eight for each row and column (or a sample of 1 in 64), a wavelet resolution of 2^4. The low frequency wavelet coefficients were inverted to reconstruct the image as before. For this analysis pixel maps have been prepared so that the information can be compared more directly. Kriged estimates were made to coincide with the original data points for each data set using the variogram model from the full set of data. These maps are also shown as pixel maps.

To evaluate the accuracy of the estimates by the wavelet reconstruction and kriging every value was compared with the original values of NIR. First the differences were calculated between the estimates and original values for both analyses and for the three sub-samples, and these are shown as pixel maps (Figures 16 and 17, 21 and 22, 26 and 27). The statistical distribution of these differences or errors has also been determined and these are shown as histograms (Figures 18, 23 and 28). In addition the mean squared differences or mean squared error (mse) was calculated (Table 3).

Results

The results were not entirely what we expected and we have been making sure that the kriging program and analyses have been correct. From the theory of geostatistics we should expect that the kriged estimates would have the smallest mse, but they do not for any of the analyses. It was this that led us to explore the differences in more detail to try to gain insight into the results from the two methods.

Sample of 1 in 2

The pixel maps for the low frequency wavelet reconstruction and kriging from the 1 in 2 data, Figures 8 and 15, respectively appear to be very similar to each other. The slight 'spottiness' evident on the kriged map is because punctual kriging was used and this is a true estimator returning the value at the data points. Table 3 gives the mean squared errors for both methods. That for the wavelets is less. The maps of errors or comparisons, Figures 16 (wavelet) and 17 (kriging), show a similar pattern in general. However, the differences between them help to explain why the mse is greater for the kriged estimates than for the wavelet reconstruction. There are large differences associated with the lakes where there are clearly marked local changes associated with boundaries in the variation. This is evidence of local non-stationarity which violates the assumptions of kriging. Wavelets are known to be suitable for dealing with local non-stationarity, and these results support this. Kriging has the largest absolute differences and there are more of them than for the low frequency wavelet reconstruction. However, compared to the number of pixels in the data these larger differences are few

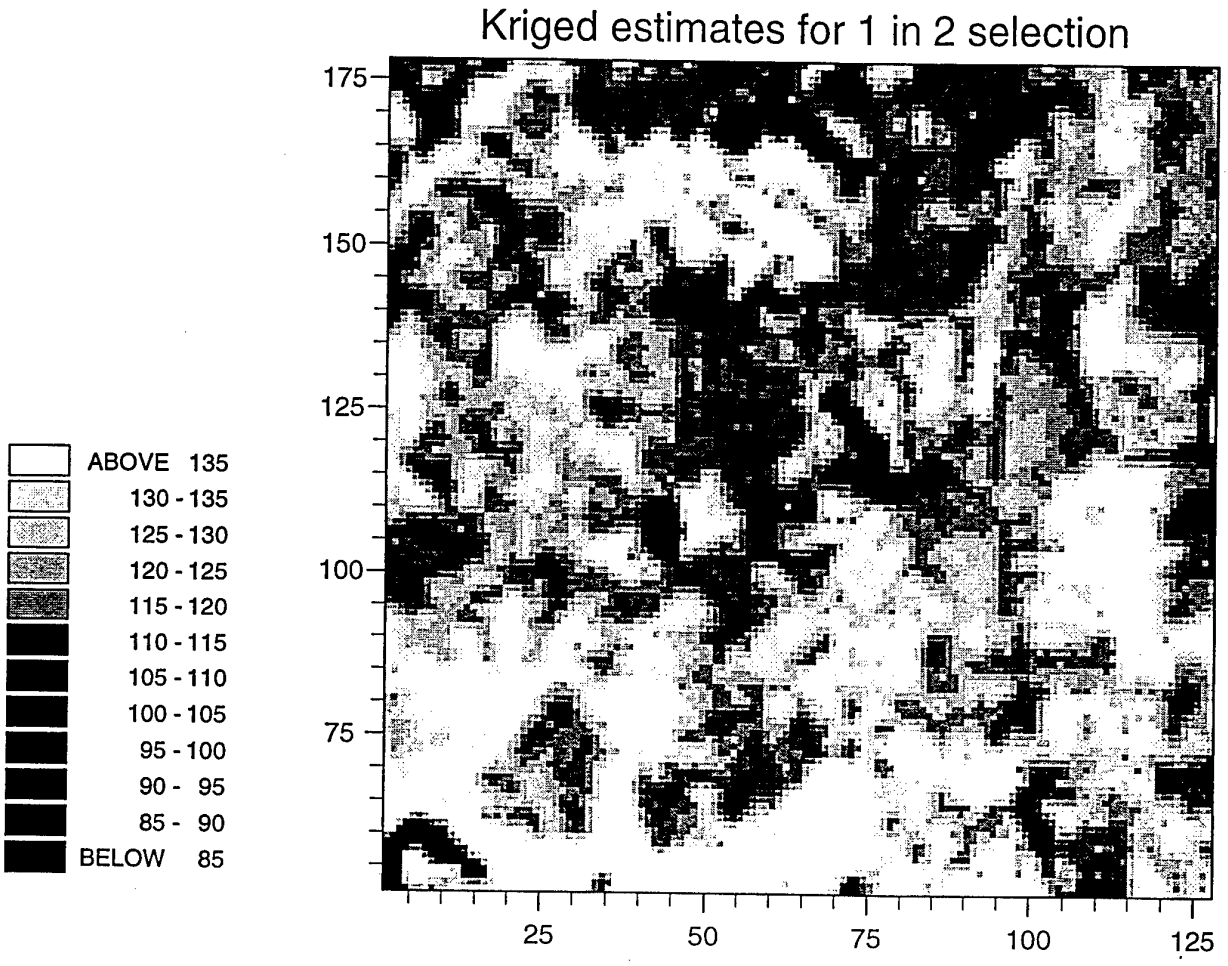

Figure 15: Pixel map of the kriged estimates for the 1 in 2 sample of NIR of part of the SPOT image (128 by 128 pixels) for Fort A. P. Hill

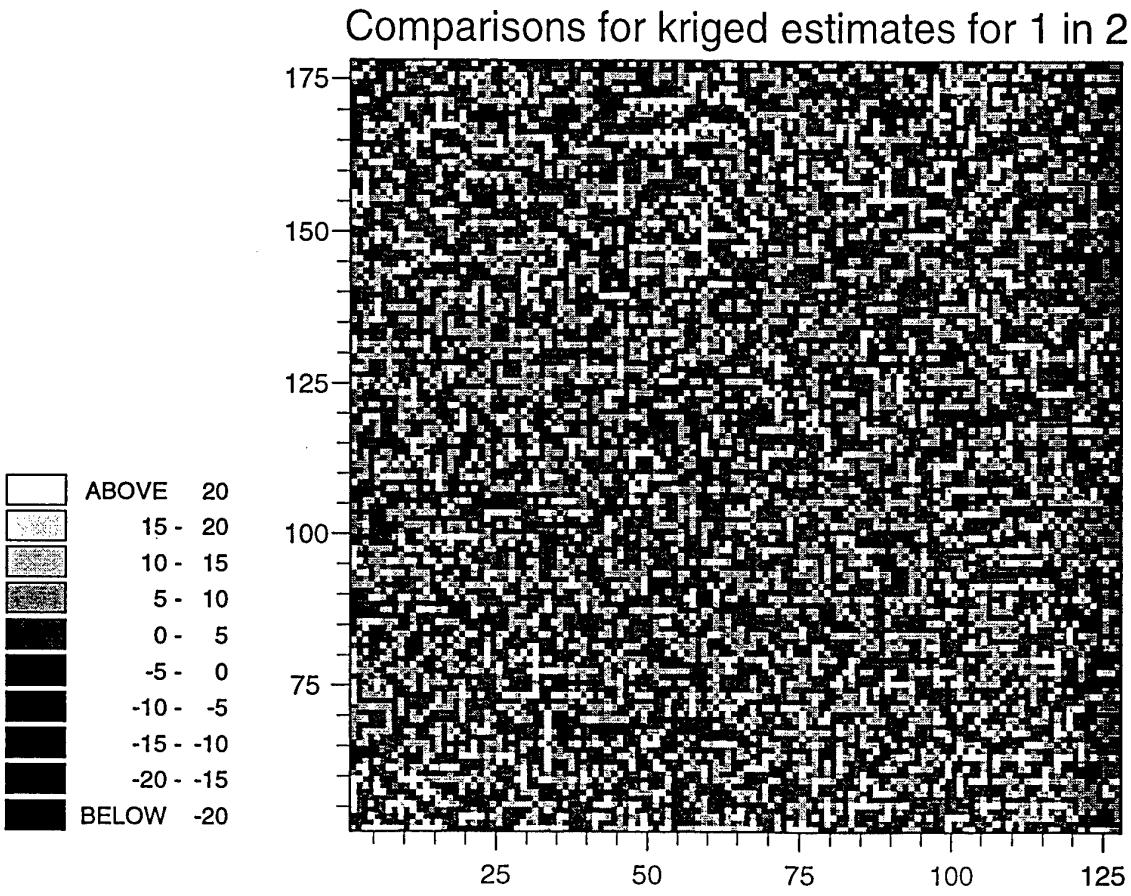

Figure 16: Pixel map of the comparisons between the kriged estimates for the 1 in 2 data with the original NIR values of part of the SPOT image (128 by 128 pixels) for Fort A. P. Hill

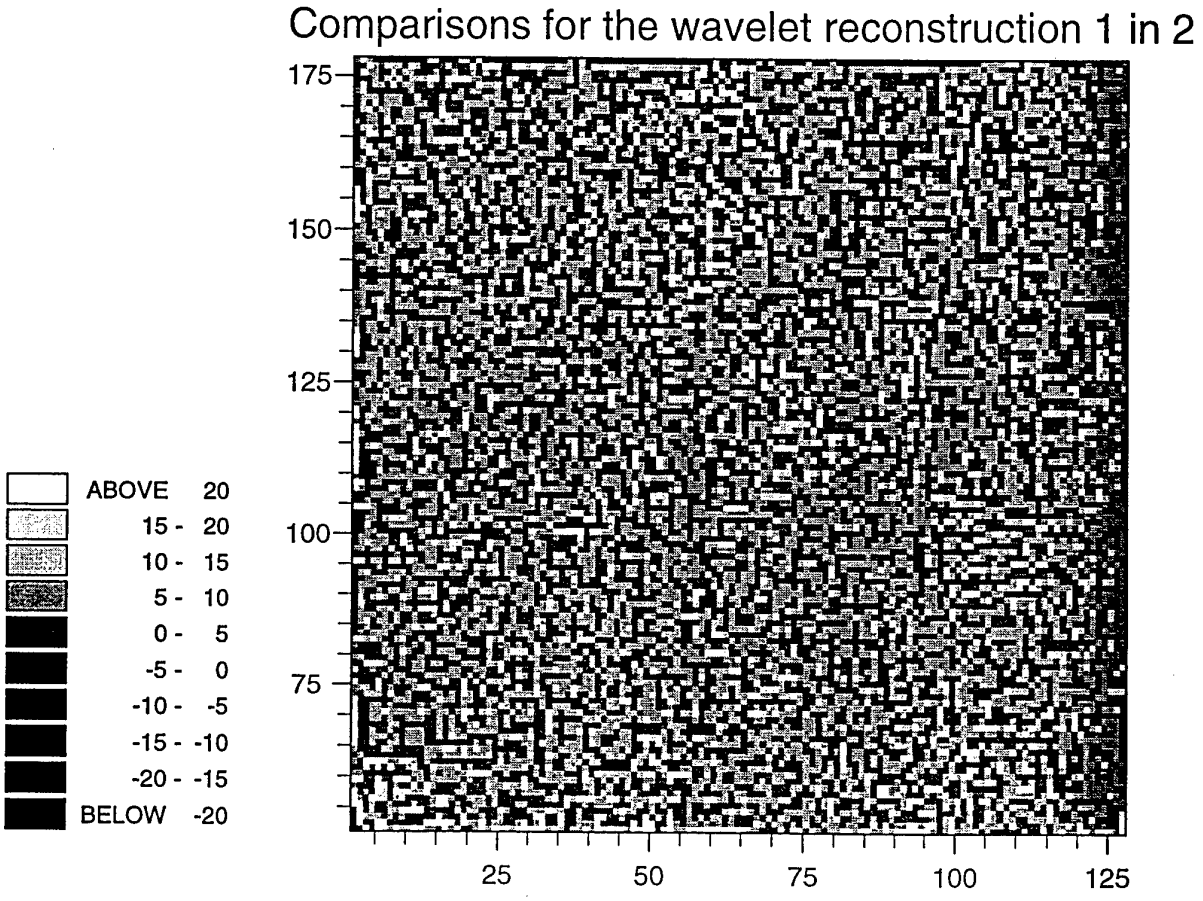

Figure 17: Pixel map of the comparisons between the low frequency wavelet reconstructed values for the 1 in 2 data with the original NIR values of part of the SPOT image (128 by 128 pixels) for Fort A. P. Hill

a)

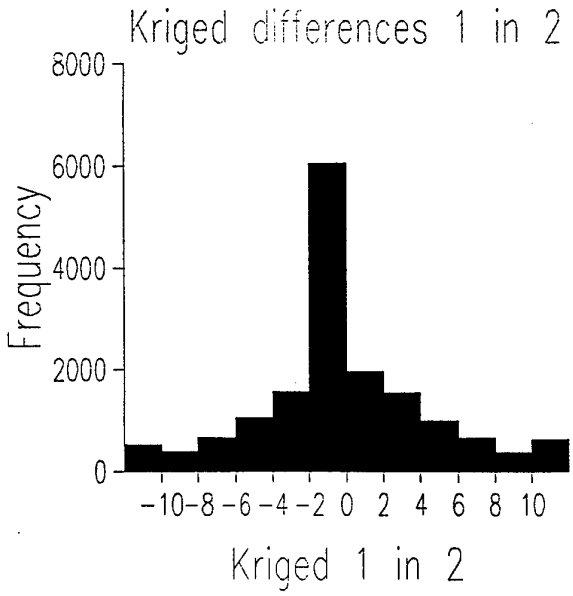

b)

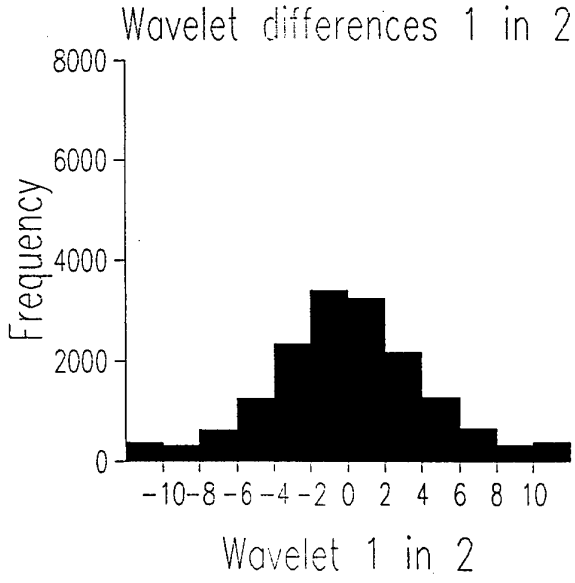

Figure 18: Histograms of a) the kriged errors and b) the wavelet errors for the 1 in 2 sampling for NIR of part of the SPOT image (128 by 128 pixels) for Fort A. P. Hill

compared with the many much smaller differences for the majority of the estimates.

To explore the reasons for the results in more detail the histograms of the differences were examined. Figure 18 a and b are the histograms of the differences for the wavelet and kriging analyses, respectively. It is clear that punctual kriging, which is a true estimator at the data points has a larger number of small errors than the wavelet analysis. However, this is not consistent as the number of data points retained is reduced.

Sample of 1 in 4

Figure 19 shows the result of kriging this sub-sample. It is evident that much of the short-range variation has been lost even though the variogram of the full data set was used. This map is similar to that for the long-range component. The map of the low frequency reconstruction, Figure 20, shows more of the short-range variation and appears to be much more accurate visually than the kriged map. The maps of the differences, Figures 21 and 22, appear to be similar overall, but closer examination shows that the patches where the differences are large for kriging are more extensive than those for the wavelet analysis. The values of the MSEs for kriging and the wavelet analysis in Table 3 also suggest that kriging performs worse than wavelets. The histograms, Figure 23a (kriging) and b (wavelets), suggest that more of the kriged values have smaller differences from the original values than those for the wavelet reconstruction. However, the number of large errors is also greater for the kriged values.

Sample of 1 in 8

Figure 24 shows the result of kriging this sub-sample. It is evident that much more of the detail in the variation has been lost. The pattern that is returned is coarse and no longer reflects even the long-range component of the variation as accurately. Figure 25 for the low frequency reconstruction from the wavelet analysis also shows how the detail has been lost. The maps of the differences, Figures 26 and 27 are again similar, but as before where the differences are greatest for the kriged differences (Figure 25) so their extent is also more extensive. It seems from the MSEs Table 3 that as the data become more sparse and separated by greater distances that kriging loses power in comparison with the wavelet analysis. The histograms, Figure 28 a (kriging) and b (wavelets), suggest that the wavelet analysis has performed better with this sub-set of the data. In the central part of the distribution there is little difference between the differences for wavelet analysis and kriging, but there seem to be many more large errors for kriging than the wavelets.

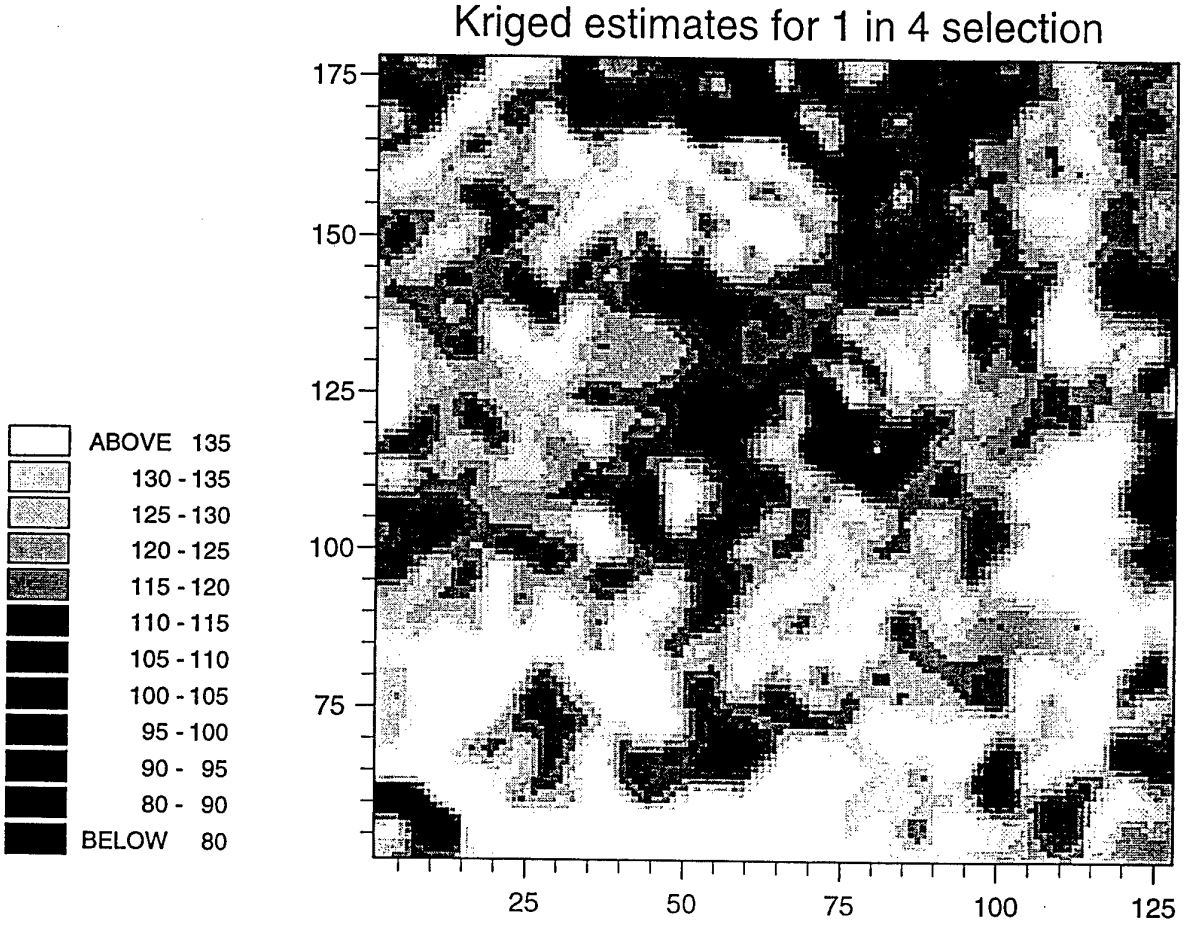

Figure 19: Pixel map of the kriged estimates for the 1 in 4 sample of NIR of part of the SPOT image (128 by 128 pixels) for Fort A. P. Hill

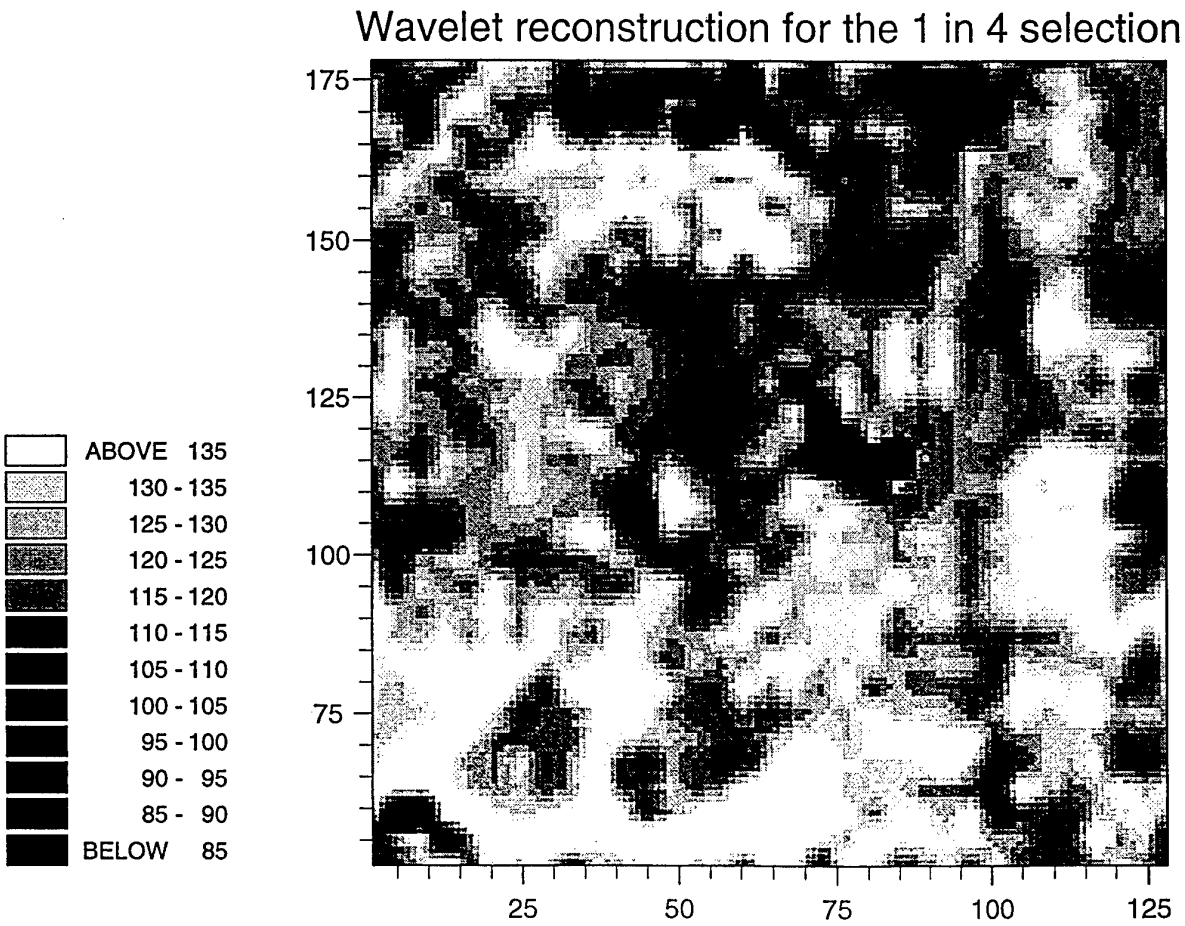

Figure 20: Pixel map of the low frequency reconstruction from the wavelet analysis of NIR of part of the SPOT image (128 by 128 pixels) for Fort A. P. Hill at a resolution of 1 in 4

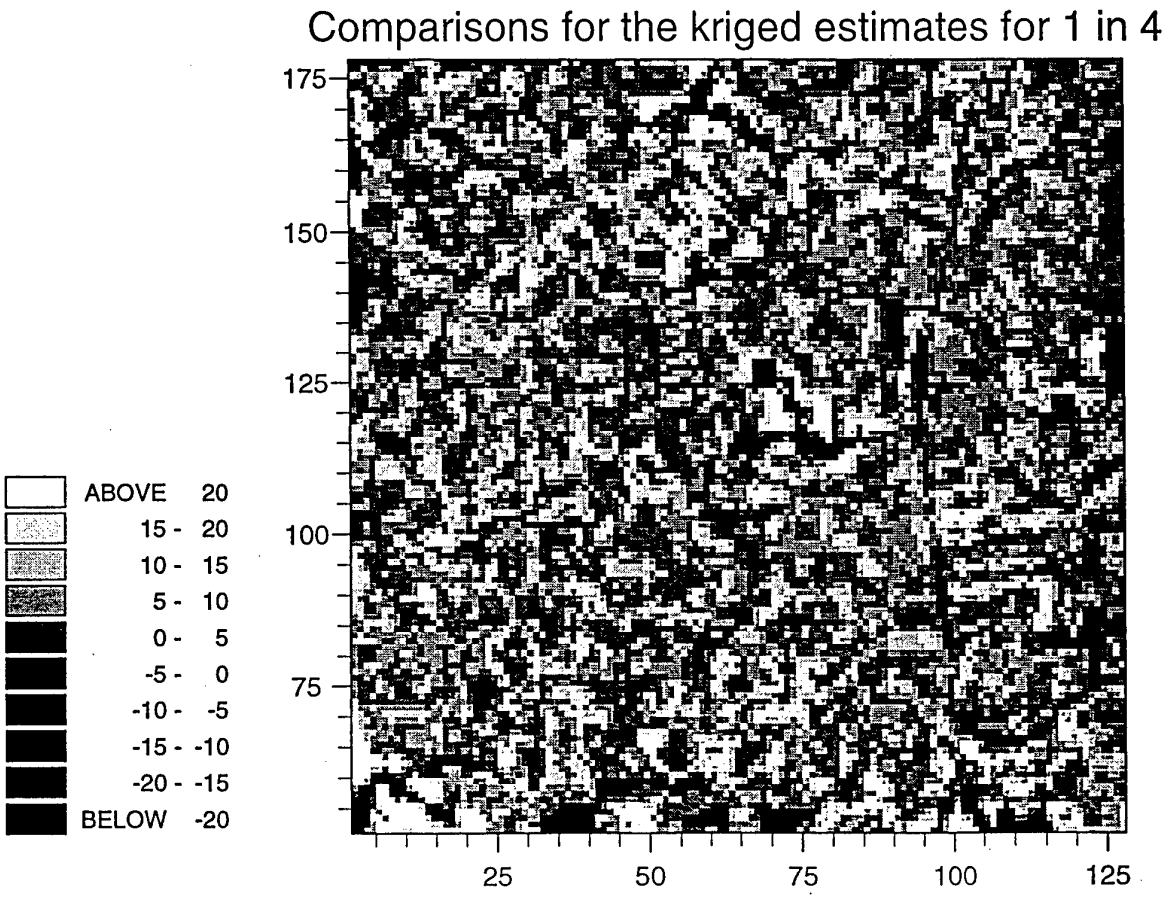

Figure 21: Pixel map of the comparisons between the kriged estimates for the 1 in 4 data with the original NIR values of part of the SPOT image (128 by 128 pixels) for Fort A. P. Hill

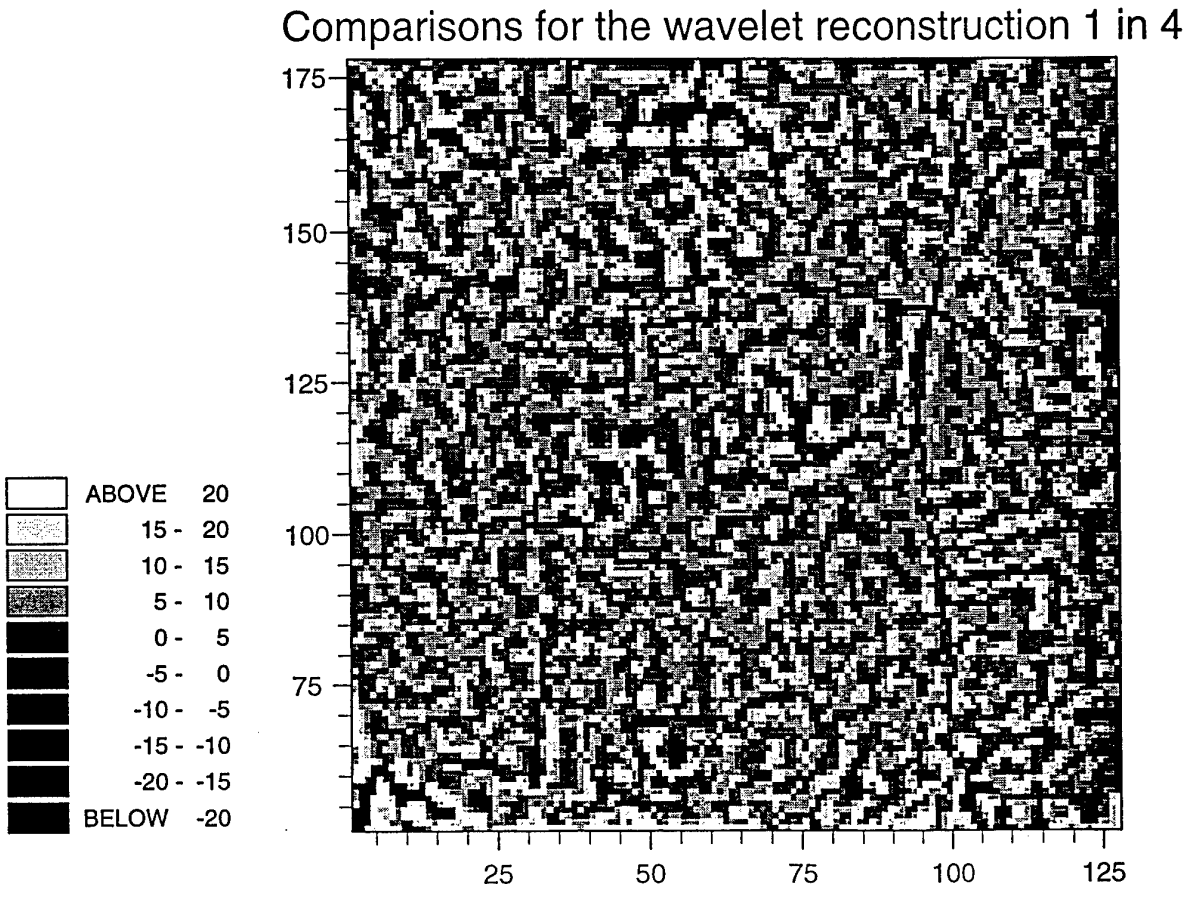

Figure 22: Pixel map of the comparisons between the low frequency wavelet reconstructed values for the 1 in 4 data with the original NIR values of part of the SPOT image (128 by 128 pixels) for Fort A. P. Hill

a)

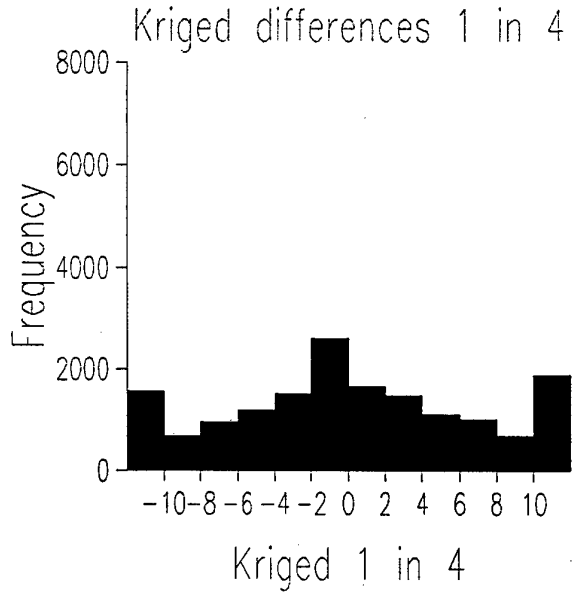

b)

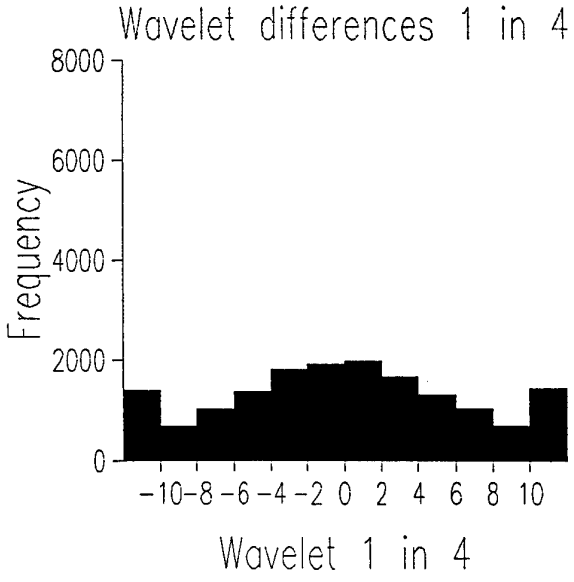

Figure 23: Histograms of a) the kriged errors and b) the wavelet errors for the 1 in 4 sampling for NIR of part of the SPOT image (128 by 128 pixels) for Fort A. P. Hill

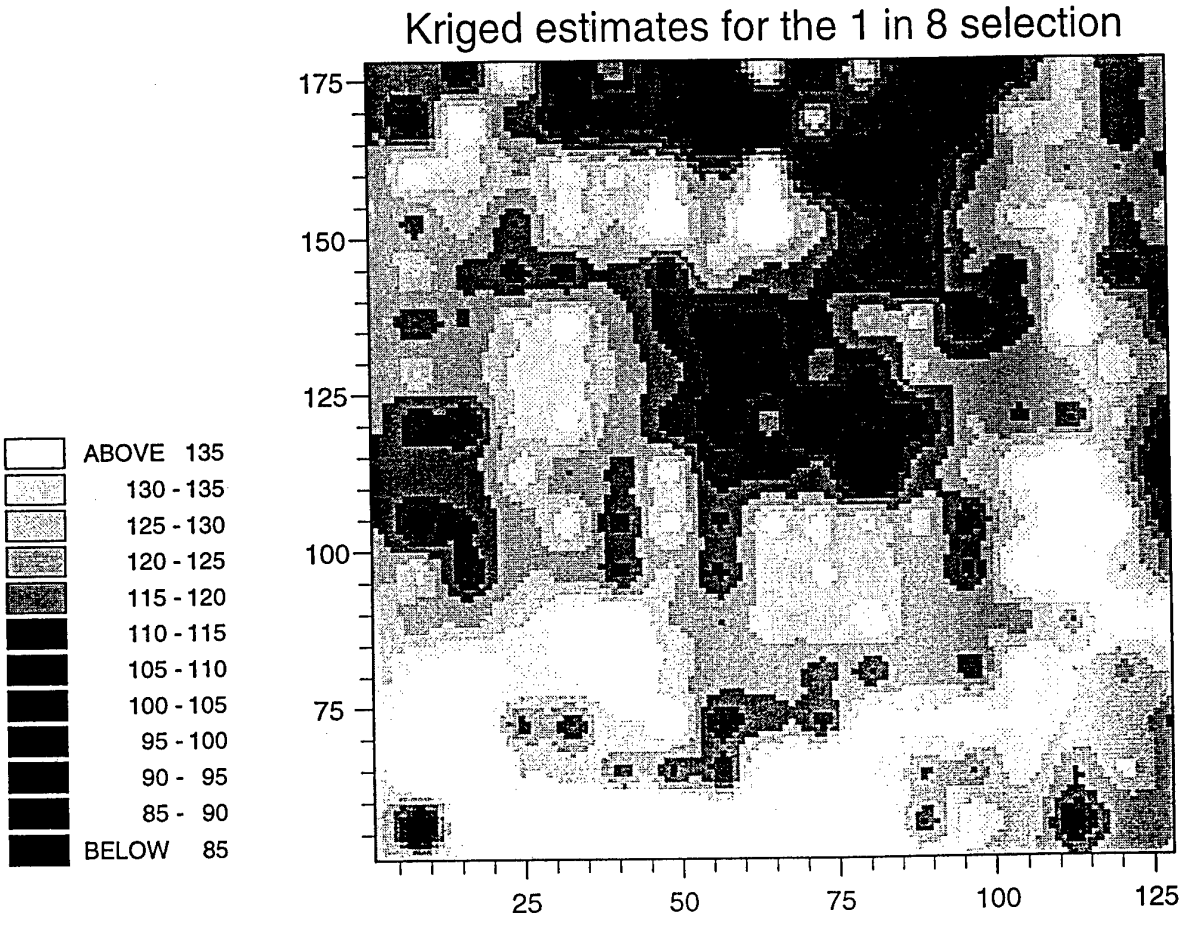

Figure 24: Pixel map of the kriged estimates for the 1 in 8 sample of NIR of part of the SPOT image (128 by 128 pixels) for Fort A. P. Hill

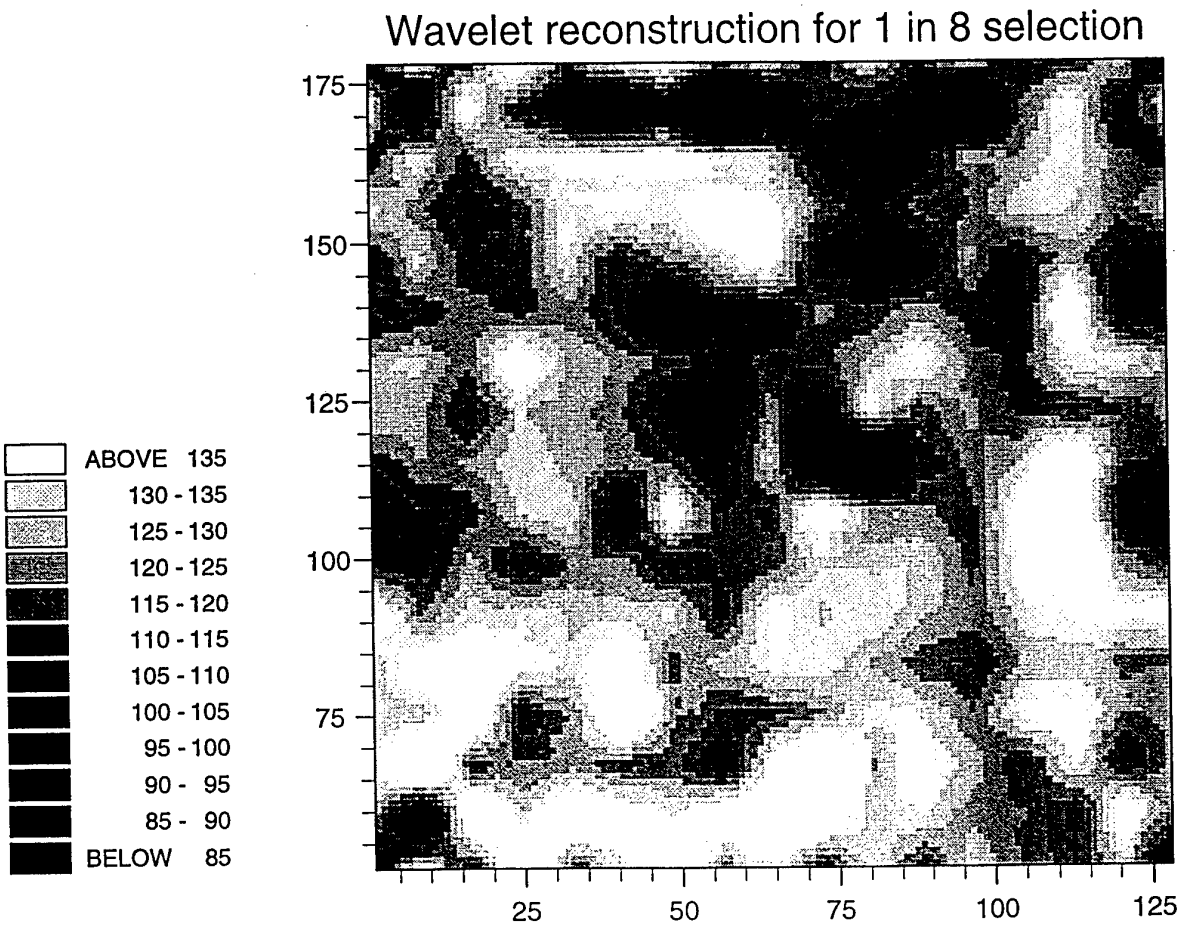

Figure 25: Pixel map of the low frequency reconstruction from the wavelet analysis of NIR of part of the SPOT image (128 by 128 pixels) for Fort A. P. Hill at a resolution of 1 in 8

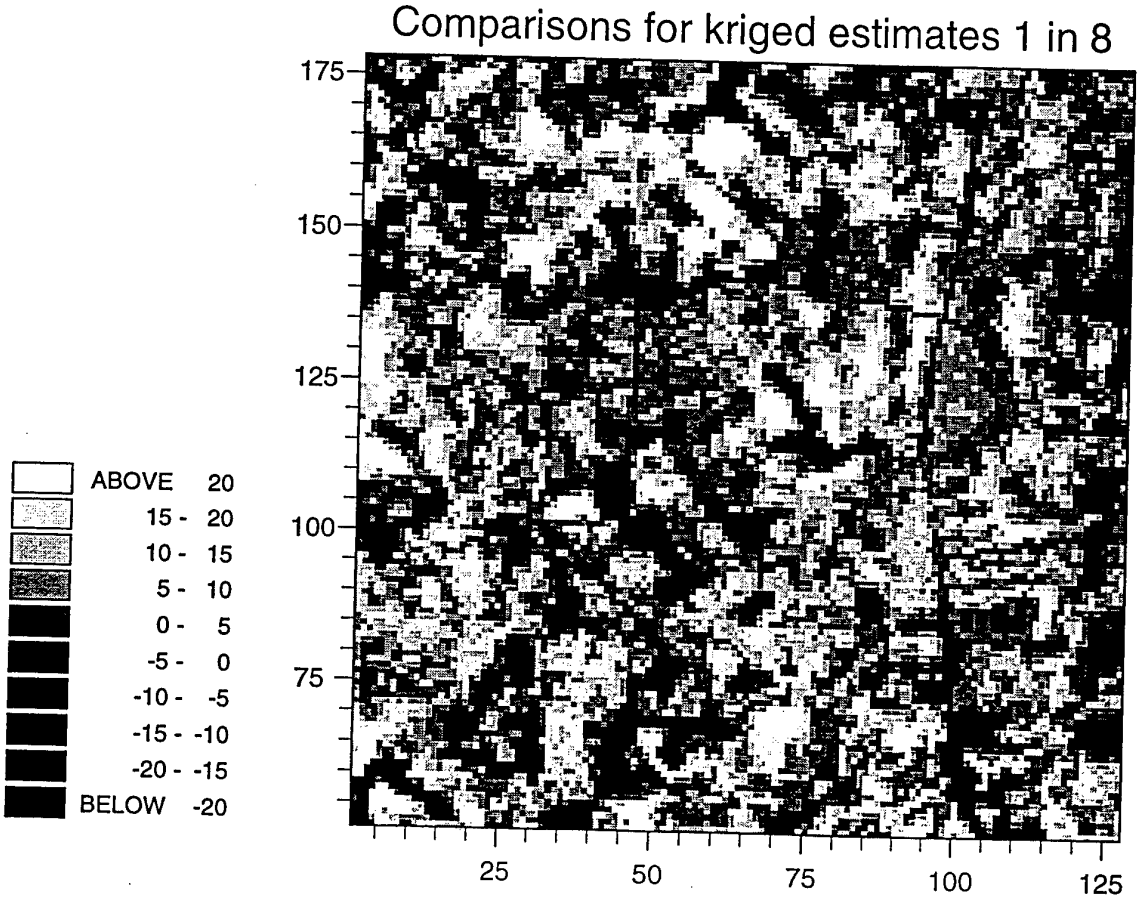

Figure 26: Pixel map of the comparisons between the kriged estimates for the 1 in 4 data with the original NIR values of part of the SPOT image (128 by 128 pixels) for Fort A. P. Hill

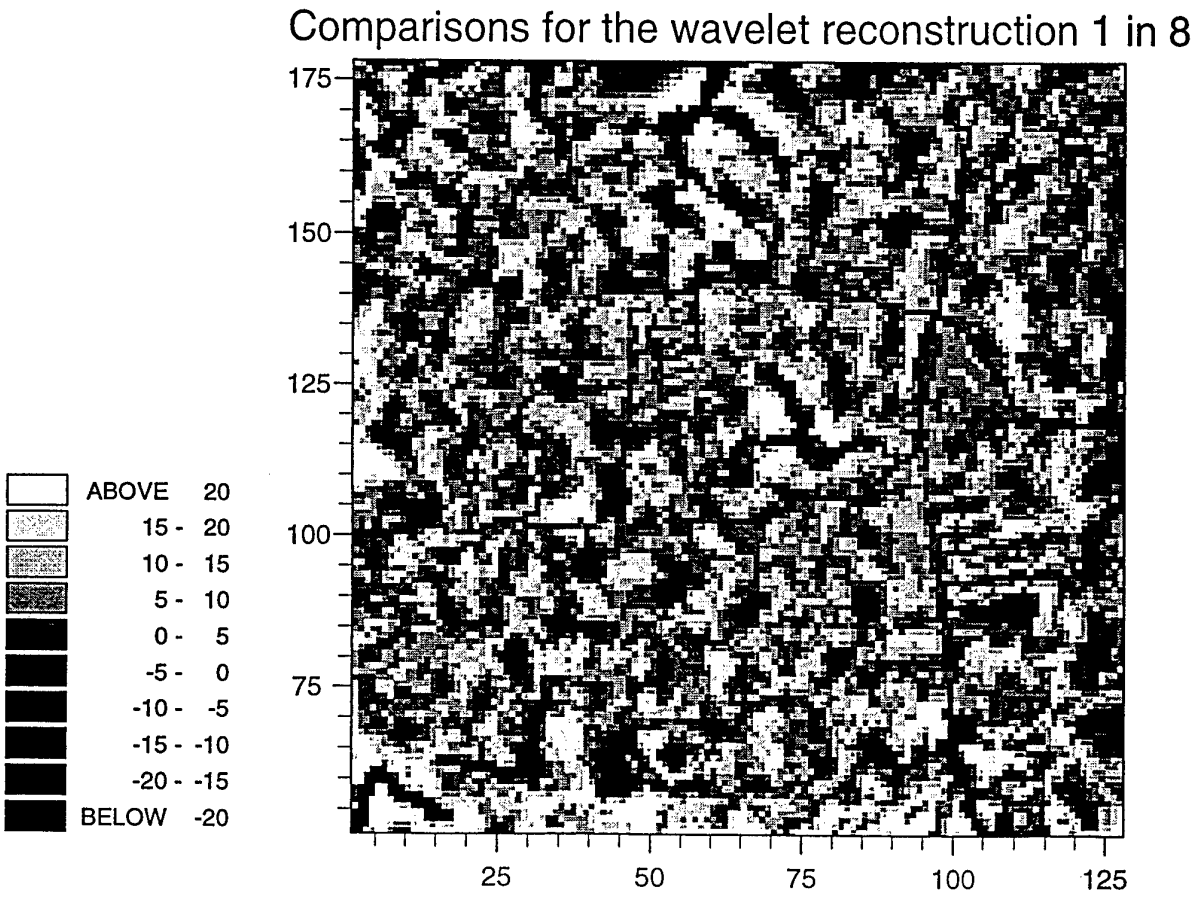

Figure 27: Pixel map of the comparisons between the low frequency wavelet reconstructed values for the 1 in 8 data with the original NIR values of part of the SPOT image (128 by 128 pixels) for Fort A. P. Hill

a)

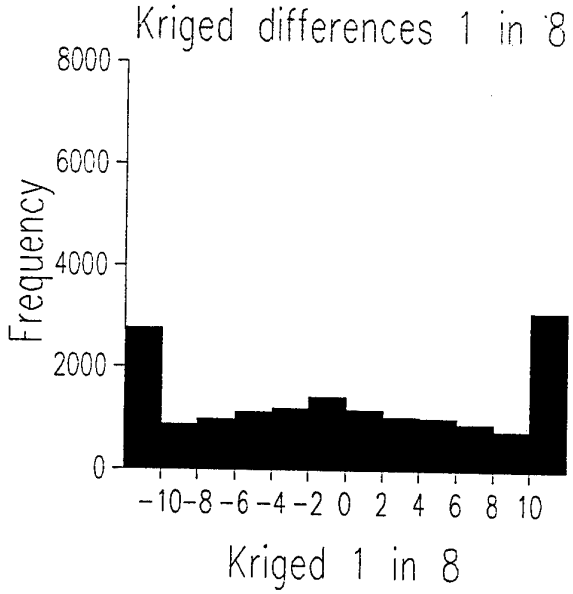

b)

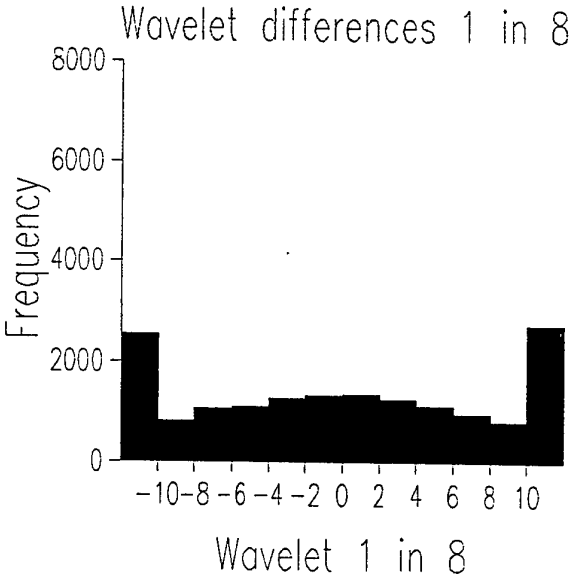

Figure 28: Histograms of a) the kriged errors and b) the wavelet errors for the 1 in 8 sampling for NIR of part of the SPOT image (128 by 128 pixels) for Fort A. P. Hill

Summary

The histograms of the differences are perhaps the most illuminating part of this analysis. It seems that we need to explore more, but that kriging performs well when fewer data have been removed than the wavelet analysis. It also suggest that the end-user can be provided with some insight to enable them to choose which is appropriate for their needs. It seems that for the 1 in 2 and 1in 4 data sub-sets more of the errors are small for kriging than for wavelets, but that the overall error is least for the wavelet analysis. The latter is clearly more successful at retaining the transition features present which kriging will not do well. Again what does the end user want?

Another thing that seems to emerge from this investigation is that the variogram could be used to choose an optimal subset of the data, based on the distance between the values. With the 1 in 2 sample both the long-range and short-range components of the variation were restored as we should expect from the correlation structures in the variogram: the distance between the pixels was less than the range of the short-range component. With the 1 in 4 sample only the long-range structure is successfully restored. If that is what is required then this can be chosen in a way that is driven by the data using the variogram.

It is interesting to note that the means of the kriged reconstructed values, Table 3, are close in each case to the mean of the original data, Table 1. The variances for the kriged values decrease as the sampling intensity decreases and is evidence of the smoothing of the variation that occurs with kriging. However, the variance of the kriged values for the 1 in 2 sample is closer to the original variance than any of the other analyses. The wavelet analysis retains the variance better as the sampling intensity decreases. Geostatistical simulation would probably perform even better in terms of retaining the variance in the data and this method should also be compared with wavelet analysis in the future.

APPENDIX I

Wavelets and Kriging for Filtering and Data Reconstruction

M. A. OLIVER[1], E. BOSCH[2] and K. SLOCUM[2]

[1]*Department of Soil Science, The University of Reading, Whiteknights, Reading RG6 6DW, UK,*
[2]*US Topograhic Engineering Center, 7701 Telegraph Road, Alexandria, Virginia 22310-3864, U. S. A.*

Abstract

Wavelet analysis operates locally and can describe a wide range of frequencies simultaneously and filter them by multi-resolution analysis. Kriging analysis also filters spatial variation at different resolutions. We compare the effectiveness of wavelets and factorial kriging for exploring nested variation in a SPOT image. In addition both wavelets and kriging can be used to restore image data after compression. We compare the reliability of the restorations from the two approaches.

The near infrared (NIR) waveband of part of a SPOT image covering Fort A. P. Hill in Virginia was used for these analyses. The region is on the dissected Piedmont area of the eastern United States. An area of 128 by 128 pixels was selected from the scene for analysis. The experimental variogram was computed and modelled by a nested spherical function with correlation structures of about 6.5 pixels and 21 pixels. The variogram and factorial kriging separated the two main spatial features present. The low-frequency component from the wavelet analysis contained the spatial structure. The long-range component became evident as the resolution decreased. The high-frequency components removed only the uncorrelated variation and we could not retrieve the short-range component.

The image was sampled so that one in every four pixels was retained, one in every 16 and one in every 64. Using the variogram model for the full set of data values were estimated at the former data points by ordinary kriging. The low-frequency wavelet transform for these resolutions was inverted so that the missing values were restored. The restored values from both analyses were compared with the original values and the mean squared differences (MSD) computed. For all resolutions the MSD was smaller for the wavelet reconstruction. However, the MSD proved somewhat misleading when frequency distributions of the errors were compared. They suggested that wavelets are more able to deal with the local fluctuations present in the image and with local non-stationarity than kriging, but that for the majority of points the kriged estimates have a smaller error.

The paper will be illustrated with maps of the results, and we shall suggest improvements for restoring images by kriging.